Research Square

Preprints are preliminary reports that have not undergone peer review.
They should not be considered conclusive, used to inform clinical practice,
or referenced by the media as validated information.

# Paenibacillus spp., a novel potato endophyte, adapts its physiology in planta to establish mutualistic symbiosis with potato

**Karmen Pogačar**

karmen.pogacar@nib.si

National Institute of Biology

**Tim Godec**

National Institute of Biology

**Juliane Albrecht**

Lund University

**Polonca Štefanič**

University of Ljubljana

**Maja Križnik**

National Institute of Biology

**Barbara Kraigher**

University of Ljubljana

**Tjaša Lukan**

National Institute of Biology

**Valentina Levak**

National Institute of Biology

**Katja Stare**

National Institute of Biology

**Marko Petek**

National Institute of Biology

**Sarah Lebeis**

Michigan State University

**Peter Dolničar**

University of Ljubljana

**Ines Mandić-Mulec**

University of Ljubljana

**Kristina Gruden**

National Institute of Biology

**Article**

**Keywords:** Potato, plant-microbe interaction, microbiome, plant-growth-promoting bacteria, bacterial adaptation, transcriptomics, endophytes, Paenibacillus

**Posted Date:** July 4th, 2026

**DOI:** https://doi.org/10.21203/rs.3.rs-9967549/v1

**License:** This work is licensed under a Creative Commons Attribution 4.0 International License. Read Full License

**Additional Declarations:** No competing interests reported.

# Abstract

Plant-associated bacteria can influence plant growth, development, and stress responses, yet the mechanisms underlying stable interactions with host plants remain incompletely understood. Here, we characterized *Paenibacillus* sp. ST1, a newly identified potato endophyte isolated from long-term maintained tissue culture plants and detected in field-grown potato. Strain ST1 efficiently colonized internal potato tissues and spread to aboveground organs, likely through the xylem, while maintaining its cellular morphology within the host. Transcriptomic analyses revealed adaptation to both root exudates and the endophytic environment, including shifts in carbon utilization, reduced expression of chemotaxis-associated genes, activation of secretion and host-interaction systems, and regulation of oxidative stress responses. In parallel, ST1-colonized plants exhibited modified root architecture consistent with improved nutrient acquisition and water use, as well as increased tolerance to potato virus Y (PVY). Strain ST1 induced plant transcriptional responses associated with microbe-triggered immunity, although at relatively mild levels consistent with a mutualistic interaction. Together, these findings provide insight into the mechanisms underlying the establishment and maintenance of a stable long-term endophytic association between bacteria and potato plants, while highlighting its contribution to plant growth promotion and stress resilience.


# Introduction

The potato (*Solanum tuberosum* L.) is one of the world's most widely cultivated staple crops, which plays a crucial role in global food security and agricultural economies (*CIP - International Potato Center, 2025)*. However, the productivity of the potato is affected by various biotic and abiotic stress factors. Biotic stress factors include diseases such as late blight (*Phytophthora infestans*), viral infections such as potato virus Y (PVY) and potato leaf roll virus (PLRV), and insect pest colorado potato beetle (*Leptinotarsa decemlineata*), which can cause up to 80% of yield losses (Islam et al., 2024). Abiotic stress factors such as drought, heat and salinity pose an additional threat to potato production and require innovative approaches to improve plant resilience and productivity (Handayani et al., 2019). Plant growth-promoting (PGP) microorganisms have emerged as promising biofertilizers due to their ability to enhance plant health through multiple mechanisms, including improved nutrient uptake, phytohormone production, induction of systemic resistance against pathogens, and mitigation of environmental stress (Ansabayeva et al., 2025). These microorganisms play a critical role in sustainable agriculture by reducing the need for chemical fertilizers and pesticides while promoting overall plant vigour and yield (Borriss, 2011; O'Callaghan et al., 2022; Veselova et al., 2022).

Among these beneficial microorganisms, endophytic microbial communities represent a promising but less studied group. These microorganisms transiently or permanently reside within plant tissues, where they establish intimate, non-pathogenic interactions with the host plant (Hallmann et al., 1997). To persist within plant tissues, endophytes must evade or modulate the plant immune system. Plants recognize conserved microbial molecules, known as microbe-associated molecular patterns (MAMPs), which activate MAMP-triggered immunity (MTI) (Jones & Dangl, 2006). Plant immune responses are

further regulated by signalling pathways involving salicylic acid (SA), jasmonic acid (JA), and ethylene, together with the production of reactive oxygen species (ROS) (Pieterse et al., 2012). To evade plant defence, endophytic bacteria typically produce MAMPs that weakly activate plant immunity and often lack or produce only low levels of effectors (Colaianni et al., 2021; Ma et al., 2021). Alternatively, they can degrade plant immunogenic peptides or produce ROS-detoxifying enzymes such as superoxide dismutase (SOD) and glutathione reductase (GR) (Ordon et al., 2025; Sessitsch et al., 2012).

Beyond successful colonization (White et al., 2019), many endophytes actively enhance plant defence against pathogens (Uwaremwe et al., 2022; Zhou et al., 2014). Like plant growth–promoting rhizobacteria (PGPR), some endophytic bacteria can enhance plant defence against pathogens by producing antimicrobial compounds (e.g. antibiotics and cell wall–degrading enzymes such as chitinases) and by priming plant immune responses through modulation of ethylene, JA and SA signalling pathways (Pieterse et al., 2014). In potato, endophytic bacteria have been shown to reduce viral disease incidence and damage caused by non-vector insect pests while inducing systemic resistance (ISR) (Sorokan et al., 2020). In addition to protection against biotic stress, endophytes can also increase plant tolerance to abiotic stresses such as drought, salinity, and extreme temperatures. They achieve this through the production of protective compounds or by altering plant physiological processes to better withstand adverse environmental conditions (Hasanović et al., 2024; White et al., 2019; Yang et al., 2024).

Among endophytic bacteria, the genus *Paenibacillus* has garnered significant research interest. Members of this genus are Gram-positive, endospore-forming bacteria that occur in diverse ecological niches, including the internal tissues of various plants (Omomowo & Babalola, 2019). These bacteria have demonstrated a strong capacity to promote plant growth through mechanisms such as nitrogen fixation, phosphate solubilization, and siderophore production. They can also enhance plant stress tolerance and suppress the growth of plant pathogens (Phi et al., 2008; Weselowski et al., 2016; Yuan et al., 2025). Despite the well-documented PGP effects of mutualistic bacteria, the underlying molecular mechanisms that enable their adaptation to the plant environment and facilitate the expression of growth-promoting functions are still not fully understood.

In this study, we identified and characterized a novel potato endophyte belonging to genus *Paenibacillus*, designated *Paenibacillus* sp. ST1. It was derived from plantlets maintained in long-term tissue culture. We explored its functional capabilities to gain insight into mechanisms behind such tight interaction. We confirmed the capability of this strain to fix atmospheric nitrogen, solubilise inorganic phosphate, produce the auxins, and enzymes involved in cellulose and hemicellulose degradation. Using GFP labelling and microscopy, we demonstrated its colonization dynamics and morphological adaptations within plant tissues. Further, we showed that the strain slows viral multiplication and improves root architecture for drought tolerance, highlighting its potential as a beneficial endophyte for sustainable plant protection strategies. Finally, we show, using transcriptome analysis, that bacteria adapt to endophytic lifestyle by reducing its chemotaxis and mobility, altering the carbon and nitrogen usage

metabolism and inducing plant communication mechanisms while moderately triggering the plant immune system.

## Methods

# Genome sequencing, assembly and annotation of bacteria

Genomic DNA (gDNA) was isolated from bacteria growing around the roots of potato plants in sterile tissue cultures in solid MS30 media (5 g of Murashige and Skoog Basal Medium with vitamins (Duchefa), 30 g of sucrose, 8g agar per 1 L of bidistilled water, pH 5.8) using the DNeasy Plant Mini Kit (Qiagen, Germany) according to the manufacturer's instructions. The 16S rRNA gene was amplified using primers Bakt_341F/ Bakt_805R (460-bp amplicon) targeting the V3–V4 region (Table S1). PCR products were purified using Wizard® SV Gel and PCR Clean-Up System (Promega) and subjected to Sanger sequencing (Eurofins Genomics). The obtained sequences were analysed using BLAST (BLASTn) (Altschul et al., 1997) against the core nucleotide NCBI database (https://blast.ncbi.nlm.nih.gov/) to determine initial taxonomic identity.

Using the isolated gDNA, we applied a combination of Oxford Nanopore (ONT) and Illumina paired-end sequencing to generate high-quality reads for bacteria genome assembly. Nanopore library prep using ligation kit SQK-LSK109 and sequencing was performed in-house on a MinION using one Flongle flow cell (r9.4.1 pores). Illumina genomic DNA libraries were prepared and sequenced by Novogene Ltd. on Illumina NovaSeq 6000 platform using 150 bp paired-end reads. Multiple independent assemblies of ONT reads were generated using Flye v2.8.3 (Kolmogorov et al., 2019), Miniasm v0.3 (H. Li, 2016), NextDenovo v2.5.0 (Hu et al., 2024), and Raven v1.6.1 (Vaser & Šikić, 2021) and combined into a consensus assembly using the Trycycler pipeline v0.5.4 (Wick et al., 2021). The consensus assembly was then polished using ONT reads with medaka v1.7.1 (ONT; https://nanoporetech.github.io/medaka/) and using Illumina reads with Polypolish v0.4.3 (Wick & Holt, 2022). Methylation was basecalled using dorado v0.9.6 (ONT; https://github.com/nanoporetech/dorado) and the super-accuracy (sup) model dna_r9.4.1_e8_sup@v3.3_5mCG@v0.1.

The quality of the generated assemblies was assessed using QUAST v5.0.2 (Mikheenko et al., 2018) and by manual inspection of read alignments to the assembled genome in IGV (Robinson et al., 2011). Genome annotation was conducted using NCBI's Prokaryotic Genome Annotation Pipeline build6021 (PGAP; Tatusova et al., 2016) and eggNOG-mapper v2.1.12 (Cantalapiedra et al., 2021) with eggNOG database v5.0.2. Secondary metabolism gene clusters were predicted using antiSMASH v8.0.1 (Blin et al., 2025) and rhizosphere-competence-related catabolic gene clusters using rhizoSMASH v0.3.1 (Y. Li et al., 2025). To identify PGPB-associated genes, the PLaBAse PGPT-Pred (Patz et al., 2021) analysis using blastp and hmmer mapper was used and genes with blastp hits below e-value threshold 1e-05 were considered reliable. Bacterial operons were predicted using two methods, Operon Mapper (Taboada et al., 2018) and OperonSEQer (Krishnakumar & Ruffing, 2022). Signal peptides for gene products were predicted using SignalP v6.0 (Nielsen et al., 2024).

Genome-based taxonomic placement was performed with the Type Strain Genome Server (TYGS; Meier-Kolthoff & Göker, 2019) using the updated database (Freese et al., 2026), applying the 70% dDDH threshold (formula $d_4$) for species delineation (Meier-Kolthoff et al., 2013), and with classify workflow of the GTDB-Tk v2.7.1 (Chaumeil et al., 2022) against GTDB release 232 (Parks et al., 2020).

**In vitro plant growth-promoting activity assays**

A range of plant growth-promoting traits of newly isolated bacterial strain were assessed, including siderophore and indole-3-acetic acid (IAA) production phosphate solubilization, nitrogen fixation, various enzymatic activities (pectinase, cellulase, chitinase, protease, xylanase), starch hydrolysis, biofilm formation, and surfactant production (Y. Liu et al., 2025; Lukan et al., 2026). Full experimental protocols for each assay are provided in the Supplementary Methods.

# Generation of stable GFP-tagged bacteria

For fluorescence visualization experiments, wild-type *Paenibacillus* sp. ST1 was genetically tagged with the $P_{upp}$-gfp cassette using Gibson assembly, which was integrated at the *amyS* locus. To construct the integration plasmid (pPSPB), five DNA fragments were amplified and assembled. The plasmid pKM8 (Doan et al., 2005) served as the backbone, from which a 3217 bp fragment was amplified using primers Pkm8_F and Pkm8_R (Table S1). The *gfp* gene, driven by the *upp* promoter, and a *chloramphenicol resistance marker gene* (*CmR*) were amplified from pAD43-25 (Dunn & Handelsman, 1999) using primers GFP_F/GFP_R and Cm_F/Cm_R, respectively (Table S1). To enable chromosomal integration at the *amyS* locus, upstream (*amyS* front) and downstream (*amyS* back) flanking regions were PCR-amplified from the bacteria using primers amyS_front_F/R and amyS_back_F/R (Table S1). Primers were designed with overlapping sequences to enable seamless fusion of fragments via the Gibson Assembly Master Mix (Thermo Scientific). The final plasmid pPSPB (Fig. S1) was extracted from *E. coli* and introduced into bacteria via electroporation (Supplementary Methods). Successful integration at the *amyS* locus resulted in stable fluorescent tagging of the strain.

# Plant material

Potato plants, including non-transgenic cv. Désirée and cv. Rywal, the SA-depleted NahG transgenic line(Baebler et al., 2014) and two independent transgenic lines with silenced RBOHD gene (shRBOHD L13, L14) (Lukan et al., 2020), all in Rywal genetic background, were used in this study. Plants were cultured for two weeks via stem node tissue culture following in vitro micropropagation under controlled environmental conditions in growth chambers PSI (Photon Systems Instruments) (day/night cycle: 22 ± 2°C/19 ± 2°C, light intensity: 70–90 µmol $m^{-2}$ $s^{-1}$ (PPFD), relative humidity: 55% ) and a 16-hour photoperiod. Potato plants transferred to soil after two weeks were grown under similar controlled environmental conditions in PSI growth chambers.

Seeds of *Nicotiana tabacum* L. cv. White Burley were germinated and grown in pots containing soil in growth chambers (PSI) (16-h photoperiod at 22 ± 2°C/19 ± 2°C (day/night), with a light intensity of 70–90 µmol $m^{-2}$ $s^{-1}$ PPFD and 55% relative humidity).

## Bacterial plant inoculation

GFP-tagged bacterial cultures were initiated by plating the bacteria on LB media with chloramphenicol (5 µg/mL) and selecting individual colonies, followed by overnight cultivation in a liquid LB medium with chloramphenicol (5 µg/mL) in a shaking incubator at 180 rpm and 28°C for 16–18 hours. The next morning, a 10% inoculum was prepared in LB medium without selection and cultured in a shaking incubator at 180 rpm and 28°C for about 3 hours until the exponential growth phase was reached. The cells were harvested by centrifugation at 4500 rpm for 10 minutes, then resuspended in a suitable solution and diluted to the desired optical density at 600 nm ($OD_{600}$) for downstream applications.

For potato root inoculation in liquid medium, the bacteria cultures were resuspended in MS30 medium to an optical density ($OD_{600}$) of 0.3. A volume of 3 mL of the bacterial culture was transferred to each well of a 12-well microtiter plate. Two-week-old potato plantlets were then placed in the wells, ensuring that their roots were fully immersed in the bacterial suspension. The plate was placed on a shaker at a low speed of 35 rpm and incubated three to 24 hours in a growth chamber for biofilm formation experiments, drought response analysis, plant phenotyping, root gene expression analysis and RNA-seq of bacteria incubated with potato plants. For plant colonization experiments and drought experiments the plants were incubated with roots immerged in bacterial culture for 3 h, then planted in soil and kept in a growth chamber under controlled conditions until further analyses. The 3 h incubation time was determined as optimal for 100% efficiency of plant inoculation in prior optimization experiments using qPCR detection of bacteria in aboveground plant tissues.

For potato root inoculation in agar medium, the bacteria were grown overnight in liquid LB medium. After incubation, the culture was centrifuged and resuspended in an equal volume of 1x MS medium supplemented with 1% sucrose. The bacterial suspension was then mixed with 1x MS medium and 1% sucrose containing agar (8 g/L) at approximately 40°C and poured into square plates for a final concentration of $10^5$ CFU/mL. After solidification, the plant apexes were transferred to the medium and kept in a growth chamber under controlled conditions. This setup was used for potato root phenotype studies.

For plant leaf inoculation, the bacteria were resuspended in MES-$MgCl_2$ infiltration medium to an $OD_{600}$ of 0.5 for bacterial transcriptome profiling (*in planta*), $OD_{600}$ of 0.2 for PVY tolerance experiments, $OD_{600}$ either 0.2 or 0.1 for bacterial morphology *in planta* experiments using confocal microscopy and $OD_{600}$ of 0.6 for bacterial morphology *in planta* experiments using TEM. Three- to four-week-old soil grown potato plants cv. Rywal or *N. tabacum* were used for infiltration. A small incision was made with a needle, and the bacterial suspension was introduced into three consecutive fully developed leaves using a syringe without a needle on the abaxial side. After bacterial infiltration, the leaves were rinsed with sterile water

to remove any bacteria remaining on the surface. The plants were then kept in a growth chamber for further analysis.

*Bacillus subtilis* PS-216 YFP was cultured as previously described (Lukan et al., 2026). Briefly, bacteria were grown overnight in LB medium with spectinomycin (100 µg/mL) at 37°C and 180 rpm. The culture was diluted to a 1% inoculum and grown to exponential phase (around 3 h), then diluted in 3 mL MS30 medium to $OD_{600}$ = 0.02 ($10^7$ CFU/mL) and transferred to 12-well plates for root biofilm formation experiments and root gene expression analysis.

## Confocal microscopy

A confocal microscope (Stellaris 5 with HC PL FLUOTAR 10x/0.30 DRY objective, Leica Microsystems) was employed to detect GFP-tagged bacteria on plant roots, leaves and stem. This imaging was part of potato tissue culture colonization experiments and bacterial morphology *in planta* experiments, where plant leaves were observed from 1 to 6 days post inoculation (dpi). GFP emission was tracked after excitation at 488 nm with detection in the 505–530 nm range. Chlorophyll fluorescence was excited at 488 nm, with emissions collected from 690 to 750 nm.

Leica TCS LSI macro confocal with ACS APO 20x objective (Leica Microsystems) was used to detect emission of YFP for *B. subtilis* PS-216 and GFP for *Paenibacillus* p. ST1 in root biofilm formation experiments three and 24 hours after onset of inoculation. YFP emission was recorded at 505–560 nm, GFP at 505–530 nm, and chlorophyll fluorescence at 690–750 nm, following excitation with a 488 nm laser.

Selected regions of interest (ROIs) were scanned unidirectionally at a speed of 400 Hz with frame average 2. Detailed imaging parameters for each experiment, including objectives, zoom settings, optical zoom, pinhole size, z-stack intervals, and magnifications, are available in the supplementary dataset deposited on Zenodo (DOI: 10.5281/zenodo.20477373). Image processing was completed with Leica LAS X software, creating maximum projections from Z-stacks across channels.

# Transmission electron microscopy (TEM)

To compare the morphology of bacteria when internalized in leaf tissue and in liquid culture, TEM with negative staining was used. Bacteria were extracted from potato leaves three days after infiltration by cutting four leaves into small strips in 20 mL sterile 0,7% NaCl solution and incubated 1–2 h on a shaker at 40 rpm at room temperature. The homogenate was transferred through a 40 µm strainer and centrifuged at 4500 rpm for 10 minutes. Supernatant was discarded and bacterial pellet was used. Pure bacterial culture, grown in LB medium until exponential growth phase ($OD_{600}$) of 0.6, was used as a control.

Pellet with bacteria was resuspended in 0.1 M phosphate buffer with 2% polyvinylpyrrolidone (Sigma Aldrich) and the suspension was applied on freshly glow-discharged copper grids (400 mesh, formvar-carbon coated, SPI) three times for 5 minutes, washed and stained with one droplet of 1% (w/v) water solution of uranyl acetate. Two grids were prepared for each sample. The grid was observed by transmission electron microscope TALOS L120C (Thermo Fisher Scientific, The Netherlands), operating at 100 kV. Micrographs (camera Ceta 16M) were taken using Velox software (Thermo Fisher Scientific).

## PVY tolerance experiments

To study bacteria-mediated protection against disease development in potato and tobacco, plants were inoculated with PVY-N605(123)-GFP (Lukan et al., 2023) three days after bacterial infiltration as described previously (Baebler et al., 2009). The formation and progression of disease symptoms was monitored by counting the lesions on each leaf and photographing the leaves until 11 days post-inoculation. For statistical analysis of lesion number on potato leaves, data were first tested for normality using the Shapiro–Wilk test. For comparisons between two groups, data that were not normally distributed were analysed using the Mann–Whitney U test. For normally distributed data with unequal variances, as indicated by the F-test, comparisons between groups were performed using Welch's unpaired t-test. Differences were considered statistically significant at $p < 0.05$. All analyses were conducted using GraphPad Prism version 10.4.2 (GraphPad Software, San Diego, CA, USA).

The spread of the virus throughout the tobacco plants was monitored using the Whole Plant Imaging System Newton 7.0 BIO (Vilber, France). GFP emission from the GFP-tagged PVY clone was monitored in the 480 nm excitation channel using the F-550 emission filter. Images were acquired using EvolutionCapt Edge x64 (Vilber). All plants were imaged with an exposure time of 50 seconds, a 10 x 10 field of view (FOV) and a focus of 1852 at five time points: 3–7 dpi.

The analysis of the viral multiplication areas on the inoculated tobacco leaves was carried out using Kuant software (Vilber, France). A series of six viral multiplication areas were measured on the uppermost fully developed inoculated leaf of six treated and six control plants. The total signal intensity was determined as the sum of the gray values within the region of interest (ROI) and is proportional to the intensity and spread of the GFP signal. Data collected repeatedly from the same areas over time were analysed using a mixed-effects model, with treatment and time as fixed factors and area as a random factor. Šídák's multiple comparisons test was used for post-hoc analysis. Differences were considered significant at $p < 0.05$. All analyses were conducted using GraphPad Prism version 10.4.2 (GraphPad Software, San Diego, CA, USA).

## Plant phenotyping

Root development of plants growing in MS10 medium with bacteria at $10^5$ CFU/mL was followed for three weeks by photographing the plates using a LED light panel. Root length was measured using

ImageJ software (Schneider et al., 2012), with graph paper included in the images as a scale reference. Statistical significance was determined by one-way ANOVA followed by Šídák's multiple comparisons test, performed in GraphPad Prism version 10.4.2 (GraphPad Software, San Diego, CA, USA).

Drought response analysis was performed by inoculating potato roots for 3 h with strain ST1 or MS30 medium (control), as described above. Plants were subsequently transferred to soil and, from the second week of growth onwards, maintained under reduced soil moisture conditions (< 20% volumetric water content, VWC). Plant height was measured once per week. Statistical significance was determined using an unpaired t-test with Welch's correction in GraphPad Prism version 10.4.2.

Plant volume of *RbohD* and SA-deprived potato genotypes was determined using a phenotyping platform (Photon Systems Instruments, PSI). Plants were inoculated as described above, transferred to nutrient-depleted soil, and imaged once weekly for five weeks. Plant volume was estimated from RGB images captured from both top and side views. Statistical analysis was performed using a mixed-effects model (REML), with treatment and time as fixed effects and individual plant as a random effect, using GraphPad Prism version 10.4.2.

# Bacterial colonization of potato plants with bacteria in a growth chamber

After one week in soil, aboveground tissues of bacteria-root-inoculated potato plants were sampled (1st internode + leaf, 2nd internode + leaf, 3rd internode + leaf, 4th internode + leaf and apex), frozen in liquid nitrogen and stored at -80°C. gDNA from aboveground tissue samples was isolated by MagMAX™ Plant DNA Isolation Kit (Thermo Fisher Scientific) according to the manufacturer's protocol with prior homogenization using FastPrep-24 homogenizer (MP Biomedicals) in lysis buffer using FastPrep tubes. Isolated gDNA concentration and purity was assessed using NanoDrop One spectrophotometer (Thermo Fisher Scientific).

# Colonization of potato plants with bacteria in field trials

Two cultivation systems were included in the potato field colonization experiment: organic (EKO) and conventional (CON), following the designation used in the field trial. Field management practices are described in the accompanying Zenodo dataset (DOI: 10.5281/zenodo.20477373). In the conventional fields, herbicide was applied once, after planting before emergence, fungicides 6–8 times per season, and insecticides 2–3 times per season. In contrast, no synthetic herbicides or fungicides were used in the organic fields, and only insecticide certified for organic production was applied once. Fertilization in the conventional fields consisted of a farmyard manure (30 t/ha) before ploughing and a basal application of NPK (6–12–24) at 708 kg/ha, followed by a supplemental application of calcium ammonium nitrate (KAN) at 200 kg/ha. In the organic fields, a farmyard manure at a rate 40 t/ha was applied before ploughing and after potato emergence an Azocor organic fertilizer was applied at 200 kg/ha. Root and leaf tissues from both cultivation systems were collected two times per season, at early tuber initiation stage and at later tuber bulking stage. Root and leaf samples were cut in half, with one

portion surface-sterilized by immersion in 70% ethanol for 1 min followed by 1% NaOCl for 10 min and three rinses in autoclaved water, while the other portion remained non-sterilized. Samples were then frozen in liquid nitrogen and stored at − 80°C until gDNA isolation. To determine bacteria abundance in potato field colonization experiments gDNA from root and leaf samples was isolated by MagMAX™ Plant DNA Isolation Kit (Thermo Fisher Scientific) as described above. DNA concentration and purity were evaluated as stated above. Relative copy numbers of PaeniV3V4 from newly isolated bacteria were determined and normalized to relative copy numbers of *StNPR1* (a single copy gene; Petek et al., 2014). The standard curve method was used for relative gene expression quantification using quantGenius (Baebler et al., 2017).

# qPCR analysis of potato gene expression

For root gene expression analysis two-week-old potato plantlets were placed in wells containing MS30 suspensions of *Paenibacillus* p. ST1, *B. subtilis* PS216, flg22 peptide, or MS30 medium (control), ensuring that the roots were fully immersed. Flagellin 22 (Eurogentec; AS-62633) (Flg22) was prepared as 1 µM solution (Sano et al., 2014) in MS30 medium. Plates were incubated in a growth chamber on a shaker at 35 rpm for 3–24 h prior to root sampling. Approximately 50 mg of root samples were quickly frozen in liquid nitrogen and stored at -80°C. Samples were homogenized in lysis buffer using FastPrep-24 homogenizer (MP Biomedicals). RNA was isolated using RNeasy Plant Mini Kit (Qiagen) according to the manufacturer's protocol and DNAse treated using RNase-Free DNase Set (0.5 µL of DNase I per µg RNA; Qiagen). Concentration and purity of DNase-treated total RNA was evaluated using NanoDrop One spectrophotometer (Thermo Fisher Scientific) and agarose gel electrophoresis, and reverse-transcribed using the High-Capacity cDNA Reverse Transcription Kit (Thermo Fisher Scientific). All qPCR reactions were performed in 5 µl volumes in duplicates and two dilutions (10- and 50-fold) per sample using FastStart Universal Probe Master Mix (Roche). The expression of 13 genes in roots (*StACO2* ,*StPTI5, St13LOX, StRBOHD, StPR1B, StBGLU, StHSP70, StARF2, StERF1, StCAT1, StCALS, StTRXH, StStRD29*) involved in different steps of immune signalling (see Table S2 for a full list of genes and their description) was determined and normalized to the expression of two validated reference genes, *StCOX* and elongation factor 1 (*StEF*-1).

# RNA-seq analysis of bacterial transcriptome

Bacteria for RNA-seq analysis were sampled in three growth conditions: in exponential stage of growth in rich MS30 media, in the same media but in coculture with potato plants and *in planta*. For RNA-seq of bacteria in medium, bacteria were collected from liquid culture in the exponential growth phase ($OD_{600}$ = 0.5). For RNA-seq of bacteria incubated with plants the liquid bacterial culture was collected after 24 hours of coculture with potato plants (roots emerged into media with bacteria as for plant inoculation with bacteria). In both studies the bacterial culture was fixed in RNAprotect Bacteria Reagent (Qiagen) at a 5:1 ratio, immediately mixed thoroughly to ensure effective penetration of the fixative into bacterial cells, and quickly frozen in liquid nitrogen. The fixed bacterial cultures were stored at -80°C. RNA from pure bacterial culture was isolated as described in (Pšeničnik et al., 2024), with few minor changes. Instead of 0.8 mL of fixed culture, we used 1 mL of fixed culture. The culture was pelleted before lysis.

RNA was eluted after 10 min incubation with pre-warmed (80°C) RNAse-free water. Two days after potato leaf infiltration with bacteria the infiltrated leaves were harvested and stored at – 80°C. Inoculated leaves were homogenized with FastPrep-24 homogenizer (MP Biomedicals). RNA was isolated using ZymoBIOMICS RNA MiniPrep Kit (Zymo Research) according to the manufacturer's protocol or using RNeasy Mini Plant kit (Qiagen) as described above for roots, DNase treated (Qiagen) and cleaned with RNA Clean & Concentrator kit (Zymo Research).

Next, isolated ribosomal plant and bacterial RNA was codepleted using RiboCop rRNA Depletion Kits for Plants and for Bacteria (both Lexogen). Up to three ribodepletion reactions were combined and concentrated with RNA Clean & Concentrator kit (Zymo Research). Integrity of RNA was checked by TapeStation system using High Sensitivity RNA ScreenTape (Agilent). RNA was reverse-transcribed using the High-Capacity cDNA Reverse Transcription Kit (Thermo Fisher Scientific).

Ribodepleted RNA was sequenced using strand-specific RNA-seq library and 150 bp paired-end sequencing on Illumina NovaSeq X Plus platform at Novogene Inc. Four samples per treatment group were sequenced. Data quality control was performed using FastQC v0.11.9(Andrews, 2010) and centrifuge v1.0.4 (Kim et al., 2016). Adapter, N-trimming filtering reads below PHRED score 20 was performed using Trim Galore v 0.6.7 (Krueger et al., 2021). QC reports were generated using MultiQC v1.29 (Ewels et al., 2016). STAR v2.7.10b was used to map RNA-seq reads to the bacterial genome with PGAP annotation. For differential expression (DE) analysis, low expressed genes were removed and three methods implemented in R were used to identify DE genes: 1) edgeR v4.4.2 TMM normalisation followed by voom linear model fit with sample weights (voomLmFit; R. Liu et al., 2015), 2) edgeR TMM normalisation followed by negative-binomial quasi-likelihood fit (glmQLFit; Chen et al., 2025), and 3) DESeq2 library v1.46.0 (Love et al., 2014). Genes with Benjamini Hochberg adjusted p-value below 0.05 by all three methods were considered significantly differentially expressed.

# Results

### Paenibacillus sp. SP1 genome reveals gene clusters associated with endophytic lifestyle

We isolated *Paenibacillus* sp. SP1 from sterile potato tissue cultures (cvs. Désirée and Rywal) maintained in our lab for more than two decades. This bacterium occasionally occurred in media around the roots, more frequently when plants were exposed to stress conditions (Fig. S2). The microorganism was identified as a bacterium belonging to the genus *Paenibacillus* based on 16S rRNA gene amplicon sequencing (Table S2). This bacterium is a gram-positive, facultative anaerobic, endospore-forming bacterium. Based on this identification, a species-specific qPCR assay was designed (Table S2). Interestingly, the *Paenibacillus* sp. ST1 was detected in 17% of sterile potato tissue cultures (both root and shoot samples) and in all analysed potato plants after transfer to soil (100% of root and 33% of shoot samples).

The surprising fact, that this bacterium species remained present in apparently sterile potato tissue culture for several generations, led us to further examine its physiology and functional interactions with

potato plant, where it appears to exist as a stable long-term endophyte. We first performed whole genome sequencing of the bacterium using combination of Oxford Nanopore and Illumina technology. The assembled genome has the size of 6.89 Mbp with 46.14% GC content. The PGAP annotation pipeline predicted 6246 gene models, among these 6024 protein-coding genes, 86 pseudogenes, 33 rRNAs and 103 tRNAs. We identified 98.65% complete and 0.68% partial BUSCO genes, confirming the completeness of the genome.

Both taxonomic classification tools (TYGS and GTDB-Tk) placed strain ST1 within the genus *Paenibacillus* but did not match it to any described species. The closest type-strain genome in TYGS was *P. marchantiae* BMpBG1 (dDDH $d_4$ = 62.7%, 95% CI 59.8–65.5); all remaining dDDH values were ≤ 55.6% (Supplementary Information deposited on Zenodo; DOI: 10.5281/zenodo.20477373), well below the 70% species threshold, and strain ST1 formed a separate cluster in the Genome Blast Distance Phylogeny (GBDP). The GC content differed from that of *P. marchantiae* BMpBG1 by only 0.11 percentage points, ruling out sequence contamination as a source of the low dDDH. GTDB-Tk assigned the isolate to the genus *Paenibacillus* but could not assign it to a species, as no reference genome met the species-level ANI and alignment-fraction criteria.

Several secondary metabolite clusters were identified by antiSMASH. These include a cluster for production siderophores, post-translationally modified peptides such as lanthipeptides, lassopeptides, and proteusins, and several non-ribosomal peptide clusters (Fig. 1; Table S3). In addition to these, using rhizoSMASH, we identified several clusters dedicated to degradation of xylan, transporter systems for sucrose and fructose and metabolism of amino acids (Fig. 1; Table S3) that might be utilised for plant exudate exploitation or colonisation of plant tissues. PLaBAse identified genes putatively involved in auxin synthesis and export, i.e. *amiE* amidases, *aldH/dhaS* aldehyde dehydrogenases, *ysnE* acetyltransferases, and auxin symporters. Specific phosphorus solubilisation genes, e.g. *phnD/E*, *acuI/yhdH* and *phoA*, were also identified. Of particular interest, the genome contains the PGPB-associated gene *solA* involved in metabolism of Solanoeclepin A, a root-exuded compound from potato (Abedini et al., 2025).

Confirming activity of some of the clusters identified in the genome, strain ST1 exhibited multiple plant growth–promoting traits. The strain produced indole-3-acetic acid (IAA), solubilized phosphate, fixed nitrogen, and secreted a range of hydrolytic enzymes, including xylanases, cellulases, pectinases, amylases, and proteases (Fig. S3). These activities suggest that ST1 has the potential to enhance plant growth and nutrient availability.

**Paenibacillus sp. ST1 efficiently colonizes internal plant tissues**

To understand the colonisation pattern and movement of the bacterial isolate in plant tissue, we prepared GFP-tagged *Paenibacillus* sp. ST1. As many PGP bacteria form biofilms (Haque et al., 2020), we first studied the potential of strain ST1 for biofilm formation. Strain ST1 was not forming biofilm in liquid media or on potato roots of different potato genotypes (Désirée, Rywal, NahG-Rywal). No biofilm formation by strain ST1 was detected after 3 or 24 h of root incubation (Fig. 2a, middle), whereas *B.*

*subtilis* PS-216, included as a biofilm-forming control, formed extensive biofilms on plant roots (Fig. 2a, right). Instead, individual cells of strain ST1 were distributed along the entire root length and adhered to the root surface of all tested potato genotypes already after 3 h (Fig. S4).

To study the spread of stain ST1 within the plant, we transferred ST1 root-inoculated plantlets to soil and examined different tissues by confocal microscopy from 1 to 6 days post inoculation. Individual bacterial cells entered the upper parts of the plant through the vascular tissue, particularly through xylem (Fig. 2b). The bacterial cells were already visible in the petiole of the first leaf 24 h after inoculation, 48 h after inoculation they migrated through the stem to the petiole of the second leaf, and 72 h after inoculation they were already visible in the upper part of the stem (Fig. S5). To quantify the presence of strain ST1 more precisely, we collected different parts of the plants, from the lower leaves to the apical bud, and performed qPCR analysis (Fig. 2c). The results showed the presence of ST1 in all tissues collected from all treated plants. The highest relative abundance of bacterial cells was in the lower part of the plant and progressively decreased towards the apical bud. However, it should be noted that, besides vascular migration, some bacterial migration may have occurred along external plant surfaces. To rule out the natural presence of strain ST1, non-inoculated control plants were included, in which strain ST1 levels were below the limit of quantification (LOQ).

To determine whether the morphology of bacteria changes when residing in plant tissue, as it does for *B. subtilis* (Lukan et al., 2026), we performed two complementary experiments. First, we infiltrated potato leaves and observed the bacterial cells over a period of 1 to 10 days after infiltration. Confocal microscopy analysis revealed no noticeable changes in the size or shape of the bacteria during the observation period (Fig. 2d, Fig. S6). The bacterial cells were predominantly localized in the intercellular space of the lower epidermis, at the cell-cell interfaces of the spongy mesophyll cells and near or within the stomata (Fig. S6). To further confirm these results, we compared the morphology of ST1 from liquid cultures with the morphology of bacteria extracted from leaf homogenates three days after infiltration using transmission electron microscopy (TEM). The results showed no differences in shape or size of the bacteria living in two different environments (Fig. 2e).

**Colonization by Paenibacillus sp. ST1 changes dynamically during plant development**

To evaluate the abundance of newly isolated potato endophyte in field conditions we performed extensive field trials. The presence of strain ST1 was evaluated in root and leaf tissues collected from field-grown potato plants in years 2022 and 2023 during two growth stages: early tuber initiation (TI) and late tuber bulking (TB). The study compared two cultivation systems: organic (EKO) and conventional (CON) and eight different potato cultivars. The fields in years 2022 and 2023 were not the same due to crop rotation but were in proximity, therefore soil conditions were similar in both years.

Overall, approximately 85% of root samples and 44% of potato leaf samples were positive for strain ST1 (above the limit of detection, LOD) (Fig. S7a). The bacterium was detected more frequently and with higher abundance in roots than in leaves across all treatments and years (Fig. S7a). Detection rates were higher in 2022 (Fig. S7a), whereas bacterial abundance was substantially higher in 2023, particularly in

the CON cultivation system (Fig. S7b). This pattern was also associated with greater plant vigour in 2023 compared with 2022 (Fig. S7c). The strain ST1 presence was typically higher in samples collected at the late (TB) sampling period (Fig. S7a). Interestingly, no statistically significant effect of the potato cultivar or agricultural management on the ST1 abundance was detected (Fig. S7b).

The bacteria were present in sterilized leaf and root samples, indicating internal colonization. However, their abundance was the highest in non-sterilized roots (Fig. S8a,b). The abundance of strain ST1 in non-sterilized roots was lower in the late TB stage compared to early TI stage, with significant difference in year 2022 ($p = 0.0001$; Kruskal-Wallis test), while in leaves higher levels were observed in late stage compared to early stage (Fig. S8b). This suggests a dynamic colonization pattern over the course of plant development.

**Paenibacillus sp. ST1 alters potato root architecture and enhances drought tolerance**

To examine the potential benefits that the strain ST1 could be providing to the plant, we tested its effects on root growth and development. Bacteria were mixed into MS medium, while the control medium (MS) was without bacteria. The shoots were placed on the agar MS medium, and the plants were kept in a vertical position in the growth chamber. We observed that plants grown in the presence of bacteria developed a statistically higher number of roots, together with shorter primary roots (Fig. 3a; Fig. S9ab). This phenotype is consistent with enhanced IAA activity, as elevated auxin levels are known to stimulate lateral root formation while inhibiting primary root elongation (Ivanchenko et al., 2008). To examine whether the observed root phenotype depends on the presence of metabolically active bacteria, heat-inactivated bacteria were mixed into media. No differences in root architecture were observed between plants grown on media containing heat-inactivated bacteria compared to the control (Fig. 3bc). We next tested whether direct bacterium–root contact is required to modulate root architecture by applying strain ST1 as localized inoculum spots to the growth medium at the bottom of the plate, away from plant roots. No changes in phenotype were observed (Fig. S9c), indicating that exchange of metabolites is not sufficient for the observed phenotype. To complement these results, we exposed soil grown potato plants to drought. Under low soil moisture conditions (< 20% soil humidity), plants inoculated with strain ST1 exhibited enhanced drought tolerance, as indicated by significantly higher plant height compared to non-inoculated plants (Fig. 3d).

**Paenibacillus sp. ST1 colonisation improves plant tolerance to viral infection**

Next, we designed an experiment to test disease protection potential of strain ST1. We introduced bacteria in the potato NahG-Rywal leaves by infiltrating with bacterial suspension at concentration $2x10^7$ CFU/mL. NahG plants, which are deficient in SA accumulation, are sensitive to PVY and thus allow assessment of bacterial and viral behaviour under compromised SA-dependent defence responses. Two days after bacterial inoculation we infected the leaves with PVY-N605(123)-GFP. Leaves treated with the strain ST1 showed significantly lower number of lesions and improved physiological parameters compared to bacteria-untreated PVY-infected controls (Fig. 3ef, Fig. S9d). To confirm that the observed effect resulted from the interaction between the bacteria and the plant rather than from bacterial growth

medium components alone, potato leaves were infiltrated with cell-free bacterial culture filtrate obtained by removing bacterial cells from the growth medium by filtration. No significant difference in disease symptoms development was observed between the control and the filtrate-treated leaves, indicating that the protective effect requires the presence of living bacteria (Fig. 3g). To further confirm our findings, we performed a similar experiment on *Nicotiana tabacum*. Viral multiplication areas in the third treated leaf of each plant were monitored from 3 to 7 dpi using a whole-plant imaging system detecting GFP fluorescence in treated leaves. The results showed a statistically significant difference in the viral multiplication area across all imaging days (Fig. 3h). The plants that were infiltrated with the strain ST1 prior PVY infection showed smaller multiplication areas and lower mean total GFP fluorescence intensity (Fig. 9e). These findings suggest that strain ST1 limits lesion development, viral multiplication and spread, thereby conferring a protective effect against viral infection.

**Root colonization by Paenibacillus sp. ST1 specifically modulates potato gene expression**

To assess early plant transcriptional response upon initial root–bacteria contact, we exposed plant roots to the strain ST1, bacterial flagellin fragment flg22 and the biofilm-forming *B. subtilis* PS-216. Flg22 was used as a canonical inducer of microbe-triggered immunity (MTI), whereas *B. subtilis* PS-216 served as a Gram-positive rhizobacterial reference strain that robustly colonizes potato roots through biofilm formation. This comparison allowed us to determine whether ST1 elicits a typical root-associated bacterial immune response or a more muted transcriptional profile consistent with endophytic compatibility. We selected genes marking response of different signalling pathways: StRBOHD (respiratory burst oxidase homolog D), StCALS (callose synthase), and StTRXH (thioredoxin H) for ROS, St13-LOX (13-lipoxygenase) for JA, StPR1B (pathogenesis-related protein 1B) and StBGLU2 (β-1,3-glucanase / beta-glucosidase 2) for SA, StACO2 (ACC oxidase 2), StPTI5 (Pti5 ethylene-responsive ERF transcription factor) and StERF1 (ethylene response factor 1) for ethylene, ARF1 (auxin response factor 1) for auxin, and StHSP70 (heat shock protein 70) and StRD29 (responsive to dehydration 29) as abiotic stress markers. Flg22 treatment resulted in moderate induction of *StPR1B* and *StBGLU2* and some other defence markers, which is consistent with MTI response (Fig. 4a, Table S4, S5). Interestingly, strain ST1 induced even weaker responses than flg22, except for the induction of potato susceptibility gene *StPTI5* and interestingly, increased expression of the drought-responsive gene *StRD29*. *B. subtilis* PS-216 induced stronger regulation of immune and stress signalling. The expression of *StPTI5, St13-LOX, StACO2, StCALS*, and *StTRXH* was significantly higher following inoculation with *B. subtilis* than with strain ST1. Expression of *StRBOHD* was repressed only when potato roots were in interaction with *B. subtilis* (Fig. 4a, Table S4, S5). Consistent with the limited immune perturbation caused by ST1, inoculation of RBOHD-silenced and salicylic acid–depleted plants with strain ST1 did not result in detectable differences in plant growth or disease-like symptoms compared to wild-type plants (Fig. S10, S11).

**Long-term in planta colonization drives extensive metabolic reprogramming**

To identify mechanisms underlying the interaction of strain ST1 with potato plant we performed RNA-seq analysis of strain ST1 at two stages: after 24 h co-incubation with potato plant roots ('root exudates' samples) and after two days of *in planta* inhabitation (*in planta* samples) and compare it to the bacterial culture in control media (control samples). Sensing of plant root exudates in media triggered upregulation of 203 genes and downregulation of 208 genes (adj. p-value < 0.05, |logFC| > 1) (Table S6). Genes involved in invertase activity, galactose/starch–sucrose metabolism, and oxidative pentose phosphate pathway were downregulated, which suggests a reduced use of complex carbohydrates. In contrast, genes associated with amino acid biosynthesis, including *serC*, *cysE*, and *argH*, and NADP-dependent glutamate dehydrogenase, were upregulated, while expression of serine deamination (SDS) was reduced (Table S6). These metabolic changes are indicating increased nitrogen assimilation and anabolic activity. Multiple alcohol and aldehyde dehydrogenase genes, such as *adhE* and *frmA*, were strongly induced, while the acetate kinase *ackA* was downregulated. Furthermore, *bacA*/*bcrC* and other pyrophosphate-processing genes were upregulated, which suggests increased envelope maintenance and stress-response activity. Interestingly, bacterial chemotaxis genes also showed slight downregulation in response to co-cultivation with plant roots (Fig. 4d, Table S6).

Obtaining enough bacterial reads from the *in planta* samples was challenging. Even after performing depletion of both plant and bacterial rRNA, only approximately 0.5% (1.6–3.4 mio) reads uniquely mapped to the assembled strain ST1 genome, whereas in the *in-culture* samples more than 50% (227.2–300.7 mio) reads mapped. However, the transcriptional adaptation of strain ST1 to *in planta* colonization was more pronounced than to root exudates only (Table S6). KEGG pathway mapping indicated strong physiological reprogramming of bacteria *in planta* (Fig. 4b-f, Table S6). ABC transporter systems for phosphate, amino acids, carbohydrates, and metal ions were strongly induced *in planta*, indicating increased nutrient uptake and adaptation to the nutrient conditions within leaf tissue (Fig. 4b). Pathways for metabolizing starch/sucrose, galactose, and fructose/mannose were upregulated, suggesting that bacteria use plant-derived sugars *in planta* (Fig. S12, S13). Central carbon metabolism (glycolysis/gluconeogenesis and the TCA cycle), oxidative phosphorylation (Fig. 4c), and the pentose phosphate pathway were differentially expressed, indicating a shift in carbon usage and redox balance rather than active proliferation (Fig. S14, S15), which was further supported by upregulation of oxidative stress–related genes such as catalase (Table S6). This response was accompanied by broader downregulation of genes involved in ribosomal function, translation, DNA replication, and nucleotide metabolism. A smaller nitrogen-use signature also appeared specifically *in planta* (urea/urease and ammonium-related genes) (Table S6).

**In planta colonization activates bacterial host-interaction pathways**

Secretion and uptake systems are among the most prominent endophyte features that enable efficient interaction with the plant host or defence against microbial competitors. A type IVc pilus operon *tad* is downregulated *in planta* (Fig. 4d, Table S6). This operon encodes proteins that assemble into the Tight adherence (Tad) pilus (Imam et al., 2011), a structure that extrudes pilin filaments that are involved in surface sensing, cell adhesion, biofilm formation, and DNA uptake (Ellison et al., 2022; Hardoim et al.,

2015). Another pilus assembly protein gene paeni_NIB01_002376 is upregulated, however it resides in a locus surrounded with mostly uncharacterised genes (Table S6). An operon encoding a T7SS system is also upregulated *in planta* (Fig. 4d, Table S6). This system is frequently present in *Paenibacillus* genus and is characterized by the FHA domain gene *essC* and two WXG100 domain genes that might work as substrates of the secretion machinery or effectors (Garrett et al., 2024).

In addition, genes associated with host tissue adherence were activated, including surface adhesion proteins (SLH/S-layer and LysM/lectin-like domains) and carbohydrate-active enzymes (CAZymes) with CBM and dockerin domains (e.g. GH10, GH43, GH3) involved in plant cell wall degradation (Table S6). Related to the detected PGPB activities, also expression of IAA metabolism gene was regulated, *ysnE* and *TrpAB* genes were upregulated by root exudates, while *in planta ysnE* was strongly upregulated and *TrpAB* strongly downregulated (Fig. S3, Table S6). A non-ribosomal peptide synthetase-independent siderophore biosynthetic cluster was differentially expressed. The iuc system showed a modest upregulation, whereas the fec system and multiple siderophore-associated ABC transporter genes were strongly downregulated. Also, inositol catabolism genes were upregulated *in planta* (Table S6). Chemotaxis and mobility-associated genes (e.g. *flhA/B*, *fliP/R*, and *che/mcp*) were mostly downregulated, which suggests reduced motility after entry into leaf tissue (Fig. 4e). Transcription of some gene clusters linked to production of antibacterial compounds is downregulated (the lanthipeptide class II and paenilipoheptin) in strain ST1 *in planta*, whereas class IV synthetase, proteusin and lassopeptide biosynthesis genes are upregulated (Table S6). Additionally, sporulation-associated genes, including the master regulator *Spo0A* and *YhcN/YlaJ* proteins, were significantly upregulated *in planta* suggesting activation of stress-adaptation and persistence mechanisms typical of host-associated bacterial lifestyles. (Fig. 4f, Table S6). Bacterial phage shock protein (PSP) genes *pspA/B/C*, *yvqH/F*, liaF/*mprA*, and *sigE*, involved in virulence-associated cell membrane stress protection (Ravi et al., 2024), and the *xkd* tailocin gene cluster is also upregulated *in planta* (Table S6).

# Discussion

Understanding the physiological interactions between plants and associated microorganisms is essential for revealing the functional potential of bacterial taxa and assessing their potential applications in sustainable agriculture. Here we studied the interaction of potato with strain ST1, a newly identified potato endophyte, isolated from tissue culture propagated potato plantlets, as a model of stable plant-microbe association. We focused on bacterial part of interaction, on the mechanisms of bacteria adaptation to *in planta* ecological niche and its communication with the plant.

We show that our strain can colonize multiple plant tissues, including roots, stems, and leaves (Fig. 2, S6, S7), which was demonstrated also for other *Paenibacillus* species (Annapurna et al., 2013; Hao & Chen, 2017; Y. Li et al., 2019). Biofilm formation during root colonisation has been described for several plant-associated bacteria, including *B. subtilis*, which forms structured biofilms on *Arabidopsis thaliana* and potato roots (Fig. 2, Allard-Massicotte et al., 2016; Lukan et al., 2026). Similarly, some *Paenibacillus* species, such as *Paenibacillus polymyxa*, have been reported to colonise plant roots through biofilm

formation as well (Timmusk et al., 2005). In contrast, our strain ST1 does not form biofilm but instead interacts with potato roots primarily through motile cells (Fig. 2). Interestingly, once associated with plant tissues, chemotaxis and motility-related genes were mostly downregulated, especially in *planta* (Fig. 4, Table S6), indicating that motility may be mainly required during the initial host contact, while inside the plant the bacteria shift toward a more sessile, host-adapted lifestyle.

Genome analysis of *Paenibacillus* sp. ST1 revealed several genetic features consistent with a plant-associated lifestyle and potential plant growth-promoting activity. These were confirmed by in vitro assays (Fig. S3) and when comparing transcriptomes of free living and *in planta* living bacteria (Table S6). Exposure to potato root exudates triggered rapid metabolic adjustments, including shifts toward preferred carbon sources, enhanced amino acid biosynthesis, and activation of detoxification pathways, consistent with previously reported early transcriptional responses of rhizobacteria to plant root exudates (Fan et al., 2012; Mavrodi et al., 2021). In contrast, *in planta* inhabitation showed a broader physiological reprogramming. Upregulation of ABC transporters involved in phosphate (*pstSCAB*), amino-acid (*glnHPQ*), and carbohydrate uptake (*malEG*, *rbsABC*), together with alternative carbon source pathways suggests increased nutrient scavenging in the leaf environment (Fig. 4b, Table S6). *In planta* induction of gene clusters involved in xylan degradation, sugar transport and amino acid metabolism, which also corresponds to hydrolytic enzyme activities detected in strain ST1 (Fig. S3), indicate the capacity of strain ST1 to utilise plant-derived substrates. Interestingly, the PGPB-associated gene *solA*, involved in metabolism of Solanoeclepin A, a potato root-exuded compound, was induced when bacteria was in contact with root exudates (Table S6). This finding suggests a potential adaptation of strain ST1 to Solanaceous plant root environments and may contribute to efficient colonisation of potato tissues, as the ability to utilize or modify Solanoeclepin A has been proposed to promote microbial persistence in the rhizosphere of Solanaceous plants (Abedini et al., 2025). Such metabolic flexibility is a common feature of rhizosphere and endophytic bacteria that rely on root exudates and plant polymers as nutrient sources (Mavrodi et al., 2021). In parallel, the downregulation of nucleotide biosynthesis and replication-related genes in our dataset is consistent with the pattern observed in *in planta* commensals reported by Nobori et al., 2022, suggesting a shift toward reduced proliferation or a more constrained growth state. Also, chemotaxis-associated genes were downregulated in endophyte strain ST1, as it was shown for some plant-associated bacteria (Nobori et al., 2022).

Strain ST1 exhibited several PGPB and plant protection-related traits. Induction of several biosynthetic gene clusters when bacteria is in contact with either root exudates or resides in plant apoplast, shows the ability of strain ST1 to produce diverse secondary metabolites which can assist in nutrient acquisition. For example, the presence of genes associated with phosphorus metabolism and solubilisation (*phnCDE, phoA*), together with our phosphorus-solubilisation assays (Fig. S3, Table S6), supports the potential of strain ST1 to enhance plant phosphorus availability, a key trait of plant growth-promoting bacteria. The regulation of auxin-associated genes (*aldH, ysnE*) during *in planta* colonization (Table S6), combined with auxin production by strain ST1 (Fig. S3) and the observed changes in root architecture (Fig. 3), supports a role for this bacterium in modulating plant development through auxin-related mechanisms. Elevated auxin levels promote the formation of lateral roots, leading to an

increased number of shorter roots, as observed in our study (Fig. 3a-c). Many beneficial microbes, including PGP rhizobacteria, are known to produce IAA or modulate auxin transport within the plant (López-Bucio et al., 2003; Spaepen & Vanderleyden, 2011). This increased root branching may ultimately benefit the plant by enhancing nutrient absorption surface area in the upper soil layer, particularly in phosphorus-limited conditions where fine lateral roots are more efficient than deeper roots (Richardson et al., 2011). Additionally, it can improve water use efficiency and consequently increase drought tolerance as showed in our study (Fig. 3) (Chieb & Gachomo, 2023). Furthermore, we show that strain ST1 inoculated plants show improved tolerance to viral infection. Replication of virus PVY and development of disease symptoms was attenuated in potato and tabacum plants (Fig. 3e-h), suggesting that strain ST1 contributes to induced systemic resistance that have been reported for several plant-associated bacteria (Jung et al., 2024). When potato roots were inoculated with strain ST1, several immunity related genes, including *StPTI5*, *St13-LOX*, *StPR1b and StGLU2*, showed mild induction (Fig. 4a). In addition, the genome of strain ST1 encodes ribosomally synthesised and post-translationally modified peptides such as lanthipeptides and lassopeptides, antimicrobial compounds that could contribute to the suppression of phytopathogens (Mokhtar et al., 2020).

Next, we checked how bacteria evade potential adverse reaction of the plant to the foreign microbe. We previously showed that potato response to inoculation with *B. subtilis* induced strong transcriptional response in roots (Lukan et al, 2026), much stronger than our *Paenibacillus* strain (Fig. 4a). This can be explained by different ecological lifestyle of the bacteria, as *B. subtilis* is primarily an epiphytic rhizobacterium. Mutualistic endophytes often induce a more moderate immune response that allows plant colonisation while still priming defence pathways. The exceptionally weak immune activation triggered by ST1, despite efficient systemic colonization, suggests that successful long-term endophytes may rely more on immune compatibility and low immunogenicity than on active immune suppression mechanisms typically associated with pathogens (Entila & Tsuda, 2025; Gallou et al., 2009). Nobori et al. (2022) demonstrated that commensal bacteria can induce plant transcriptional responses that overlap strongly with MAMP-triggered immunity.

Changes in oxidative phosphorylation, sulphur metabolism, and the pentose phosphate pathway suggest an adaptive response of bacteria to oxidative stress. It was shown that RBOHD generated ROS is toxic for many symbiotic bacteria of the plant (Nobori et al., 2022). To evade it bacteria may regulate the activity of RBOHD (Lee et al., 2020), as it is the case of *B. subtilis*, but not strain ST1 (Fig. 4). Alternate way to evade ROS was shown to be production of IAA that can detoxify ROS (Tzipilevich et al., 2021), production of which was confirmed in our strain (Fig. S3). The strong induction of catalase genes (Table S6) suggests that strain ST1 actively mitigates oxidative stress encountered within plant tissues, potentially contributing to suppression of the host ROS response. Of note, inoculation of immune deficient potato genotypes with silenced RBOHD or depleted of salicylic acid (NahG) plants with strain ST1 did not result in development of disease as shown for some Xhantomonades (Entila et al., 2024; Ordon et al., 2025), further supporting its adaptation to a mutualistic endophytic lifestyle. Also, inositol metabolism and transport related cluster was upregulated in planta (Table S6). It was shown that capability of microbe to catabolise myo-inositol is selective trait in root colonisation of proteobacteria

(O'Banion et al., 2023). In addition, several sulphur-related genes (Table S6) involved in sulphur transfer and cofactor biosynthesis were induced *in planta*, which may contribute to adaptation to the plant environment and the detoxification or utilization of plant-derived sulphur compounds (Andres-Barrao et al., 2021; Wittstock & Burow, 2010). Several systems involved in host interaction were also regulated *in planta.* The type IVc Tad pilus operon, which is associated with surface sensing, adhesion, biofilm formation (Ellison et al., 2022; Hardoim et al., 2015; Imam et al., 2011), was downregulated in planta, suggesting that these functions become less important after successful colonization of internal plant tissues. Interestingly, the operon also contains an FHA-domain protein associated with contact-dependent prey killing in other bacteria (Seef et al., 2021), which may additionally reflect reduced competitive interactions within plant tissues. In contrast, a type VII secretion system (T7SS) and additional pilus-associated genes were upregulated *in planta*, indicating activation of secretion mechanisms that may contribute to host interaction or intermicrobial competition (Garrett et al., 2024). Notably, we did not detect regulation of a type III secretion system associated genes, a key virulence determinant of many plant pathogens, which is typically absent in commensal strains but strongly induced in pathogens *in planta* (Nobori et al., 2022). Differential regulation of barnase–barstar toxin–antitoxin systems and several antimicrobial peptide biosynthetic clusters further support a role for competitive interactions within the plant environment. At the same time, induction of membrane stress-response systems, including phage shock proteins and Lia-associated regulators, suggests adaptation to host-associated envelope and oxidative stress (Ravi et al., 2024). We also detected regulation of several transporter systems when strain ST establishes in planta (Fig. 4b), which is the immunomodulation mechanism identified in *Xhantomonadales* (Ordon et al., 2025).

The observed repression of several antimicrobial and competition-associated systems in planta suggests that ST1 shifts from an environmentally competitive lifestyle toward a host-compatible persistence strategy. This transition is accompanied by metabolic adjustment, stress-response activation, and induction of host-interaction systems that facilitate survival within plant tissues. In addition, endophyte ST1 induces plant-beneficial traits, suggesting a potentially mutualistic interaction in the potato–bacterium association.

# Declarations


### Acknowledgment

We acknowledge Sara Fišer, Anja Moškrič, Anže Vozelj, Tina Arnšek, Tjaša Mahkovec Povalej, Nastja Marondini, Ana Žuran and Valentin Fischer for technical assistance and laboratory work.


### Availability of data and material

The datasets generated and analysed during this study are publicly available. Microscopy images, supplementary datasets, and associated metadata have been deposited in the Zenodo repository (DOI: 10.5281/zenodo.20477373). Transcriptomic data have been deposited in ArrayExpress under accession number E-MTAB-17132. Genome sequencing data are available in the European Nucleotide Archive

(ENA) under BioProject accession PRJEB113252 (ERP193628), including sample SAMEA122710083 (*Paenibacillus* sp.) and sequencing runs ERR17279759 (Oxford Nanopore MinION) and ERR17279757 (Illumina NovaSeq 6000).

**Author contributions**

KP, TG, TL, MP, IMM and KG conceived and designed the study. KP, TG, JA, MK, PŠ, BK, VL, PD and KS conducted the experiments and collected the data. KP, TG and MP performed the statistical analysis. KP, TG, MP and KG drafted the manuscript; MK, TL, SL and IMM provided critical revisions. All authors approved the final version of the manuscript.

**Funding**

We acknowledge the funding support received from Slovenian Research and Innovation Agency (ARIS); grants P4-0431 (programKIS), P4-0116 (programMicro), P4-0463 (programOmike), J4-3089 (Endofiti), 02040156. The authors also acknowledge ARIS for supporting research infrastructure used in this work through grant IO-0004 and the Slovenian node of Elixir for providing access to computational resources for bioinformatics.

**Ethics approval and consent to participate**

Not applicable

**Consent for publication**

Not applicable

**Competing interests**

The authors declare that they have no competing interests

# References

1. Abedini, D., Guerrieri, A., Jain, R., White, F., Koomen, J., Yang, Y., Wang, K., Kramer, G., Bouwmeester, H., & Dong, L. (2025). A Solanoeclepin A precursor functions as a new rhizosphere signaling molecule recruiting growth-promoting microbes under nitrogen deficiency. *BioRxiv*. https://doi.org/10.64898/2025.12.29.696744
2. Allard-Massicotte, R., Tessier, L., Lécuyer, F., Lakshmanan, V., Lucier, J. F., Garneau, D., Caudwell, L., Vlamakis, H., Bais, H. P., & Beauregard, P. B. (2016). Bacillus subtilis early colonization of Arabidopsis thaliana roots involves multiple chemotaxis receptors. *MBio*, *7*(6). https://doi.org/10.1128/mBio.01664-16
3. Altschul, S. F., Madden, T. L., Schäffer, A. A., Zhang, J., Zhang, Z., Miller, W., & Lipman, D. J. (1997). Gapped BLAST and PSI-BLAST: a new generation of protein database search programs. *Nucleic*

*Acids Research*, *25*(17), 3389–3402. https://academic.oup.com/nar/article/25/17/3389/1061651

4. Andres-Barrao, C., Alzubaidy, H., Jalal, R., Mariappan, K. G., de elicourt, A. Z., Bokhari, A., Artyukh, O., Alwutayd, K., Rawat, A., Shekhawat, K., ılia Almeida-Trapp, M., Saad, M. M., & Hirt, H. (2021). Coordinated bacterial and plant sulfur metabolism in Enterobacter sp. SA187-induced plant salt stress tolerance. *Proceedings of the National Academy of Sciences of the United States of America*, *118*(46), 2107417118. https://doi.org/10.1073/pnas.2107417118/-/DCSupplemental
5. Andrews, S. (2010). *FastQC: A Quality Control Tool for High Throughput Sequence Data [Online]*. Babraham Bioinformatics.
6. Annapurna, K., Ramadoss, D., Bose, P., & VithalKumar, L. (2013). In situ localization of Paenibacillus polymyxa HKA-15 in roots and root nodules of soybean (Glycine max.L.). *Plant and Soil*, *373*(1–2), 641–648. https://doi.org/10.1007/s11104-013-1825-7
7. Ansabayeva, A., Makhambetov, M., Rebouh, N. Y., Abdelkader, M., Saudy, H. S., Hassan, K. M., Nasser, M. A., Ali, M. A. A., & Ebrahim, M. (2025). Plant Growth-Promoting Microbes for Resilient Farming Systems: Mitigating Environmental Stressors and Boosting Crops Productivity—A Review. *Horticulturae*, *11*(3). https://doi.org/10.3390/horticulturae11030260
8. Baebler, Š., Krečič-Stres, H., Rotter, A., KogovŠek, P., Cankar, K., Kok, E. J., Gruden, K., KovaČ, M., Žel, J., Pompe-Novak, M., & Ravnikar, M. (2009). PVYNTN elicits a diverse gene expression response in different potato genotypes in the first 12 h after inoculation. *Molecular Plant Pathology*, *10*(2), 263–275. https://doi.org/10.1111/j.1364-3703.2008.00530.x
9. Baebler, Š., Svalina, M., Petek, M., Stare, K., Rotter, A., Pompe-Novak, M., & Gruden, K. (2017). QuantGenius: Implementation of a decision support system for qPCR-based gene quantification. *BMC Bioinformatics*, *18*(1). https://doi.org/10.1186/s12859-017-1688-7
10. Baebler, Š., Witek, K., Petek, M., Stare, K., Tušek-Žnidarič, M., Pompe-Novak, M., Renaut, J., Szajko, K., Strzelczyk-Zyta, D., Marczewski, W., Morgiewicz, K., Gruden, K., & Hennig, J. (2014). Salicylic acid is an indispensable component of the Ny-1 resistance-gene-mediated response against Potato virus y infection in potato. *Journal of Experimental Botany*, *65*(4), 1095–1109. https://doi.org/10.1093/jxb/ert447
11. Blin, K., Shaw, S., Vader, L., Szenei, J., Reitz, Z. L., Augustijn, H. E., Cediel-Becerra, J. D. D., de Crécy-Lagard, V., Koetsier, R. A., Williams, S. E., Cruz-Morales, P., Wongwas, S., Segurado Luchsinger, A. E., Biermann, F., Korenskaia, A., Zdouc, M. M., Meijer, D., Terlouw, B. R., van der Hooft, J. J. J., … Weber, T. (2025). antiSMASH 8.0: extended gene cluster detection capabilities and analyses of chemistry, enzymology, and regulation. *Nucleic Acids Research*, *53*(W1), W32–W38. https://doi.org/10.1093/nar/gkaf334
12. Borriss, R. (2011). Use of Plant-Associated Bacillus Strains as Biofertilizers and Biocontrol Agents in Agriculture. In D. Maheshwari (Ed.), *Bacteria in Agrobiology: Plant Growth Responses* (pp. 41–76). Springer Berlin Heidelberg. https://doi.org/10.1007/978-3-642-20332-9_3
13. Cantalapiedra, C. P., Hern□andez-Plaza, A., Letunic, I., Bork, P., & Huerta-Cepas, J. (2021). eggNOG-mapper v2: Functional Annotation, Orthology Assignments, and Domain Prediction at the

Metagenomic Scale. *Molecular Biology and Evolution*, *38*(12), 5825–5829. https://doi.org/10.1093/molbev/msab293

14. Chaumeil, P. A., Mussig, A. J., Hugenholtz, P., & Parks, D. H. (2022). GTDB-Tk v2: memory friendly classification with the genome taxonomy database. *Bioinformatics*, *38*(23), 5315–5316. https://doi.org/10.1093/bioinformatics/btac672
15. Chen, Y., Chen, L., Lun, A. T. L., Baldoni, P. L., & Smyth, G. K. (2025). edgeR v4: powerful differential analysis of sequencing data with expanded functionality and improved support for small counts and larger datasets. *Nucleic Acids Research*, *53*(2). https://doi.org/10.1093/nar/gkaf018
16. Chieb, M., & Gachomo, E. W. (2023). The role of plant growth promoting rhizobacteria in plant drought stress responses. *BMC Plant Biology*, *23*(1). https://doi.org/10.1186/s12870-023-04403-8
17. *CIP - International Potato Center*. (2025).
18. Colaianni, N. R., Parys, K., Lee, H.-S., Conway, J. M., Kim, N. H., Edelbacher, N., Mucyn, T. S., Madalinski, M., Law, T. F., Jones, C. D., Belkhadir, Y., & Dangl, J. L. (2021). A complex immune response to flagellin epitope variation in commensal communities. *Cell Host & Microbe*, *29*(4), 635-649.e9. https://doi.org/10.1016/j.chom.2021.02.006
19. Doan, T., Marquis, K. A., & Rudner, D. Z. (2005). Subcellular localization of a sporulation membrane protein is achieved through a network of interactions along and across the septum. *Molecular Microbiology*, *55*(6), 1767–1781. https://doi.org/10.1111/j.1365-2958.2005.04501.x
20. Dunn, A. K., & Handelsman, J. (1999). A vector for promoter trapping in Bacillus cereus. *Gene*, *226*, 297–305. http://www.
21. Ellison, C. K., Whitfield, G. B., & Brun, Y. V. (2022). Type IV Pili: Dynamic bacterial nanomachines. *FEMS Microbiology Reviews*, *46*(2). https://doi.org/10.1093/femsre/fuab053
22. Entila, F., Han, X., Mine, A., Schulze-Lefert, P., & Tsuda, K. (2024). Commensal lifestyle regulated by a negative feedback loop between Arabidopsis ROS and the bacterial T2SS. *Nature Communications*, *15*(1). https://doi.org/10.1038/s41467-024-44724-2
23. Entila, F., & Tsuda, K. (2025). Taming of the microbial beasts: Plant immunity tethers potentially pathogenic microbiota members. *BioEssays*, *47*(1). https://doi.org/10.1002/bies.202400171
24. Ewels, P., Magnusson, M., Lundin, S., & Käller, M. (2016). MultiQC: Summarize analysis results for multiple tools and samples in a single report. *Bioinformatics*, *32*(19), 3047–3048. https://doi.org/10.1093/bioinformatics/btw354
25. Fan, B., Carvalhais, L. C., Becker, A., Fedoseyenko, D., Von Wirén, N., & Borriss, R. (2012). Transcriptomic profiling of Bacillus amyloliquefaciens FZB42 in response to maize root exudates. *BMC Microbiology*, *12*. http://www.biomedcentral.com/1471-2180/12/116
26. Freese, H. M., Meier-Kolthoff, J. P., Sardà Carbasse, J., Afolayan, A. O., & Göker, M. (2026). TYGS and LPSN in 2025: A Global Core Biodata Resource for genome-based classification and nomenclature of prokaryotes within DSMZ Digital Diversity. *Nucleic Acids Research*, *54*(D1), D884–D891. https://doi.org/10.1093/nar/gkaf1110

27. Gallou, A., Cranenbrouck, S., & Declerck, S. (2009). Trichoderma harzianum elicits defence response genes in roots of potato plantlets challenged by Rhizoctonia solani. *European Journal of Plant Pathology*, *124*(2), 219–230. https://doi.org/10.1007/s10658-008-9407-x

28. Garrett, S. R., Higginson, A. B., & Palmer, T. (2024). Multiple variants of the type VII secretion system in Gram-positive bacteria. *MicroLife*, *5*. https://doi.org/10.1093/femsml/uqae013

29. Hallmann, J., Quadt-Hallmann, A., Mahaffee, W. F., & Kloepper, J. W. (1997). Bacterial endophytes in agricultural crops. *Canadian Journal of Microbiology*, *43*(10), 895–914. https://doi.org/10.1139/m97-131

30. Handayani, T., Gilani, S. A., & Watanabe, K. N. (2019). Climatic changes and potatoes: How can we cope with the abiotic stresses? *Breeding Science*, *69*(4), 545–563. https://doi.org/10.1270/jsbbs.19070

31. Hao, T., & Chen, S. (2017). Colonization of wheat, maize and cucumber by Paenibacillus polymyxa WLY78. *PLoS ONE*, *12*(1). https://doi.org/10.1371/journal.pone.0169980

32. Haque, M. M., Mosharaf, M. K., Khatun, M., Haque, M. A., Biswas, M. S., Islam, M. S., Islam, M. M., Shozib, H. B., Miah, M. M. U., Molla, A. H., & Siddiquee, M. A. (2020). Biofilm Producing Rhizobacteria With Multiple Plant Growth-Promoting Traits Promote Growth of Tomato Under Water-Deficit Stress. *Frontiers in Microbiology*, *11*. https://doi.org/10.3389/fmicb.2020.542053

33. Hardoim, P. R., van Overbeek, L. S., Berg, G., Pirttilä, A. M., Compant, S., Campisano, A., Döring, M., & Sessitsch, A. (2015). The Hidden World within Plants: Ecological and Evolutionary Considerations for Defining Functioning of Microbial Endophytes. *Microbiology and Molecular Biology Reviews*, *79*(3), 293–320. https://doi.org/10.1128/mmbr.00050-14

34. Hasanović, M., Hrelja, E., Hajro, A. A., Murtić, S., & Durmić-Pašić, A. (2024). Exploring the Plant Growth-Promotion Properties of Rhizospheric and Endophytic Bacteria Associated with Robinia pseudoacacia L. in Serpentine Soil. *Polish Journal of Microbiology*, *73*(4), 515–527. https://doi.org/10.33073/pjm-2024-044

35. Hu, J., Wang, Z., Sun, Z., Hu, B., Ayoola, A. O., Liang, F., Li, J., Sandoval, J. R., Cooper, D. N., Ye, K., Ruan, J., Xiao, C. Le, Wang, D., Wu, D. D., & Wang, S. (2024). NextDenovo: an efficient error correction and accurate assembly tool for noisy long reads. *Genome Biology*, *25*(1). https://doi.org/10.1186/s13059-024-03252-4

36. Imam, S., Chen, Z., Roos, D. S., & Pohlschröder, M. (2011). Identification of surprisingly diverse type IV Pili, across a broad range of gram-positive bacteria. *PLoS ONE*, *6*(12). https://doi.org/10.1371/journal.pone.0028919

37. Islam, S., Li, J., Rahman, M. A., Xie, F., Song, B., & Nie, B. (2024). Resistance to biotic and abiotic stress in potato: the origin of the genes and corresponding molecular markers. *Phytopathology Research*, *6*(1). https://doi.org/10.1186/s42483-023-00222-9

38. Ivanchenko, M. G., Muday, G. K., & Dubrovsky, J. G. (2008). Ethylene–auxin interactions regulate lateral root initiation and emergence in *Arabidopsis thaliana*. *The Plant Journal*, *55*(2), 335–347. https://doi.org/10.1111/j.1365-313X.2008.03528.x

39. Jones, J. D. G., & Dangl, J. L. (2006). The plant immune system. *Nature*, *444*(7117), 323–329. https://doi.org/10.1038/nature05286

40. Jung, J., Ahn, S., Kim, D. H., & Riu, M. (2024). Triple interactions for induced systemic resistance in plants. *Frontiers in Plant Science*, *15*. https://doi.org/10.3389/fpls.2024.1464710

41. Kim, D., Song, L., Breitwieser, F. P., & Salzberg, S. L. (2016). Centrifuge: rapid and sensitive classification of metagenomic sequences. *Genome Research*, *26*(12), 1721–1729. https://doi.org/10.1101/gr.210641.116

42. Kolmogorov, M., Yuan, J., Lin, Y., & Pevzner, P. A. (2019). Assembly of long, error-prone reads using repeat graphs. *Nature Biotechnology*, *37*(5), 540–546. https://doi.org/10.1038/s41587-019-0072-8

43. Krishnakumar, R., & Ruffing, A. M. (2022). OperonSEQer: A set of machine-learning algorithms with threshold voting for detection of operon pairs using short-read RNA-sequencing data. *PLoS Computational Biology*, *18*(1). https://doi.org/10.1371/journal.pcbi.1009731

44. Krueger, F., James, F., Ewels, P., Afyounian, E., & Schuster-Boeckler, B. (2021). FelixKrueger/TrimGalore: v0.6.7. In *Zenodo*. https://doi.org/https://doi.org/10.5281/zenodo.5127899

45. Lee, D. H., Lal, N. K., Lin, Z. J. D., Ma, S., Liu, J., Castro, B., Toruño, T., Dinesh-Kumar, S. P., & Coaker, G. (2020). Regulation of reactive oxygen species during plant immunity through phosphorylation and ubiquitination of RBOHD. *Nature Communications*, *11*(1). https://doi.org/10.1038/s41467-020-15601-5

46. Li, H. (2016). Minimap and miniasm: Fast mapping and de novo assembly for noisy long sequences. *Bioinformatics*, *32*(14), 2103–2110. https://doi.org/10.1093/bioinformatics/btw152

47. Li, Y., Li, Y., Zhang, H., Wang, M., & Chen, S. (2019). Diazotrophic Paenibacillus beijingensis BJ-18 Provides Nitrogen for Plant and Promotes Plant Growth, Nitrogen Uptake and Metabolism. *Frontiers in Microbiology*, *10*(MAY). https://doi.org/10.3389/fmicb.2019.01119

48. Li, Y., Sun, M., Raaijmakers, J. M., Mommer, L., Zhang, F., Song, C., & Medema, M. H. (2025). Predicting rhizosphere-competence-related catabolic gene clusters in plant-associated bacteria with rhizoSMASH. *Nature Communications* , *16*(1). https://doi.org/10.1038/s41467-025-63526-8

49. Liu, R., Holik, A. Z., Su, S., Jansz, N., Chen, K., Leong, H. S., Blewitt, M. E., Asselin-Labat, M. L., Smyth, G. K., & Ritchie, M. E. (2015). Why weight? Modelling sample and observational level variability improves power in RNA-seq analyses. *Nucleic Acids Research*, *43*(15). https://doi.org/10.1093/nar/gkv412

50. Liu, Y., Jia, B., Ren, Y., Xun, W., Stefanic, P., Yang, T., Miao, Y., Zhang, N., Yao, Y., Zhang, R., Xu, Z., Shen, Q., & Mandic-Mulec, I. (2025). Bacterial social interactions in synthetic Bacillus consortia enhance plant growth. *IMeta*, *4*(4). https://doi.org/10.1002/imt2.70053

51. López-Bucio, J., Cruz-Ramírez, A., & Herrera-Estrella, L. (2003). The role of nutrient availability in regulating root architecture. *Current Opinion in Plant Biology*, *6*(3), 280–287. https://doi.org/10.1016/S1369-5266(03)00035-9

52. Love, M. I., Huber, W., & Anders, S. (2014). Moderated estimation of fold change and dispersion for RNA-seq data with DESeq2. *Genome Biology*, *15*(12). https://doi.org/10.1186/s13059-014-0550-8

53. Lukan, T., Pogačar, K., Kraigher, B., Stare, K., Kovačič, T. G., Zagorščak, M., Petek, M., Stefanic, P., Vozelj, A., Levak, V., Povalej, T. M., García, J. M., Pozo, M. J., Álvarez, E., Franco-Zorrilla, J. M., Križnik, M., Baebler, Š., Mandić-Mulec, I., & Gruden, K. (2026). <scp>ERF</scp> transcription factor <scp>StPti5</scp> is a regulator of endophyte community maintenance in potato. *New Phytologist*. https://doi.org/10.1111/nph.71240

54. Lukan, T., Pompe-Novak, M., Baebler, Š., Tušek-Žnidarič, M., Kladnik, A., Križnik, M., Blejec, A., Zagorščak, M., Stare, K., Dušak, B., Coll, A., Pollmann, S., Morgiewicz, K., Hennig, J., & Gruden, K. (2020). Precision transcriptomics of viral foci reveals the spatial regulation of immune-signaling genes and identifies RBOHD as an important player in the incompatible interaction between potato virus Y and potato. *Plant Journal*, *104*, 645–661. https://doi.org/10.1111/tpj.14953

55. Lukan, T., Županič, A., Mahkovec Povalej, T., Brunkard, J. O., Kmetič, M., Juteršek, M., Baebler, Š., & Gruden, K. (2023). Chloroplast redox state changes mark cell-to-cell signaling in the hypersensitive response. *New Phytologist*, *237*(2), 548–562. https://doi.org/10.1111/nph.18425

56. Ma, K.-W., Niu, Y., Jia, Y., Ordon, J., Copeland, C., Emonet, A., Geldner, N., Guan, R., Stolze, S. C., Nakagami, H., Garrido-Oter, R., & Schulze-Lefert, P. (2021). Coordination of microbe–host homeostasis by crosstalk with plant innate immunity. *Nature Plants*, *7*(6), 814–825. https://doi.org/10.1038/s41477-021-00920-2

57. Mavrodi, O. V., McWilliams, J. R., Peter, J. O., Berim, A., Hassan, K. A., Elbourne, L. D. H., LeTourneau, M. K., Gang, D. R., Paulsen, I. T., Weller, D. M., Thomashow, L. S., Flynt, A. S., & Mavrodi, D. V. (2021). Root Exudates Alter the Expression of Diverse Metabolic, Transport, Regulatory, and Stress Response Genes in Rhizosphere Pseudomonas. *Frontiers in Microbiology*, *12*. https://doi.org/10.3389/fmicb.2021.651282

58. Meier-Kolthoff, J. P., Auch, A. F., Klenk, H.-P., & ¨ Oker, M. G. (2013). Genome sequence-based species delimitation with confidence intervals and improved distance functions. *BMC Bioinformatics*, *14*, 60. http://www.biomedcentral.com/1471-2105/14/60

59. Meier-Kolthoff, J. P., & Göker, M. (2019). TYGS is an automated high-throughput platform for state-of-the-art genome-based taxonomy. *Nature Communications*, *10*(1). https://doi.org/10.1038/s41467-019-10210-3

60. Mikheenko, A., Prjibelski, A., Saveliev, V., Antipov, D., & Gurevich, A. (2018). Versatile genome assembly evaluation with QUAST-LG. *Bioinformatics*, *34*, i42–i50. https://doi.org/10.1093/bioinformatics/bty266

61. Mokhtar, N. F. K., Hashim, A. M., Hanish, I., Zulkarnain, A., Raja Nhari, R. M. H., Abdul Sani, A. A., Abbasiliasi, S., Ariff, A., Mustafa, S., & Rahim, R. A. (2020). The Discovery of New Antilisterial Proteins From Paenibacillus polymyxa Kp10 via Genome Mining and Mass Spectrometry. *Frontiers in Microbiology*, *11*. https://doi.org/10.3389/fmicb.2020.00960

62. Nielsen, H., Teufel, F., Brunak, S., & von Heijne, G. (2024). SignalP: The Evolution of a Web Server. In F. Lisacek (Ed.), *Protein Bioinformatics. Methods in Molecular Biology* (Vol. 2836, pp. 331–367). Humana, New York. https://doi.org/10.1007/978-1-0716-4007-4_17
63. Nobori, T., Cao, Y., Entila, F., Dahms, E., Tsuda, Y., Garrido-Oter, R., & Tsuda, K. (2022). Dissecting the cotranscriptome landscape of plants and their microbiota. *EMBO Reports*, *23*(12). https://doi.org/10.15252/embr.202255380
64. O'Banion, B. S., Jones, P., Demetros, A. A., Kelley, B. R., Knoor, L. H., Wagner, A. S., Chen, J.-G., Muchero, W., Reynolds, T. B., Jacobson, D., & Lebeis, S. L. (2023). Plant myo-inositol transport influences bacterial colonization phenotypes. *Current Biology*, *33*(15), 3111-3124.e5. https://doi.org/10.1016/j.cub.2023.06.057
65. O'Callaghan, M., Ballard, R. A., & Wright, D. (2022). Soil microbial inoculants for sustainable agriculture: Limitations and opportunities. *Soil Use and Management*, *38*(3), 1340–1369. https://doi.org/10.1111/sum.12811
66. Omomowo, O. I., & Babalola, O. O. (2019). Bacterial and fungal endophytes: Tiny giants with immense beneficial potential for plant growth and sustainable agricultural productivity. *Microorganisms*, *7*(11). https://doi.org/10.3390/microorganisms7110481
67. Ordon, J., Logemann, E., Maier, L. P., Lee, T., Dahms, E., Oosterwijk, A., Flores-Uribe, J., Miyauchi, S., Paoli, L., Stolze, S. C., Nakagami, H., Felix, G., Garrido-Oter, R., Ma, K. W., & Schulze-Lefert, P. (2025). Conserved immunomodulation and variation in host association by Xanthomonadales commensals in Arabidopsis root microbiota. *Nature Plants*, *11*(3), 612–631. https://doi.org/10.1038/s41477-025-01918-w
68. Parks, D. H., Chuvochina, M., Chaumeil, P. A., Rinke, C., Mussig, A. J., & Hugenholtz, P. (2020). A complete domain-to-species taxonomy for Bacteria and Archaea. *Nature Biotechnology*, *38*(9), 1079–1086. https://doi.org/10.1038/s41587-020-0501-8
69. Patz, S., Gautam, A., Becker, M., Ruppel, S., Rodríguez-Palenzuela, P., & Huson, DH. (2021). PLaBAse: A comprehensive web resource for analyzing the plant growth-promoting potential of plant-associated bacteria. *BioRxiv*. https://doi.org/10.1101/2021.12.13.472471
70. Petek, M., Rotter, A., Kogovšek, P., Baebler, Š., Mithöfer, A., & Gruden, K. (2014). Potato virus y infection hinders potato defence response and renders plants more vulnerable to Colorado potato beetle attack. *Molecular Ecology*, *23*(21), 5378–5391. https://doi.org/10.1111/mec.12932
71. Phi, Q.-T., Park, Y.-M., Ryu, C.-M., Park, S.-H., & Ghim, S.-Y. (2008). Functional identification and expression of indole-3-pyruvate decarboxylase from Paenibacillus polymyxa E681. *Journal of Microbiology and Biotechnology*, *18*(7), 1235–1244.
72. Pieterse, C. M. J., Van der Does, D., Zamioudis, C., Leon-Reyes, A., & Van Wees, S. C. M. (2012). Hormonal Modulation of Plant Immunity. *Annual Review of Cell and Developmental Biology*, *28*(1), 489–521. https://doi.org/10.1146/annurev-cellbio-092910-154055
73. Pieterse, C. M. J., Zamioudis, C., Berendsen, R. L., Weller, D. M., Van Wees, S. C. M., & Bakker, P. A. H. M. (2014). Induced systemic resistance by beneficial microbes. *Annual Review of Phytopathology*,

*52*, 347–375. https://doi.org/10.1146/annurev-phyto-082712-102340

74. Pšeničnik, A., Slemc, L., Avbelj, M., Tome, M., Šala, M., Herron, P., Shmatkov, M., Petek, M., Baebler, Š., Mrak, P., Hranueli, D., Starčević, A., Hunter, I. S., & Petković, H. (2024). Oxytetracycline hyper-production through targeted genome reduction of Streptomyces rimosus. *MSystems*, *9*(5). https://doi.org/10.1128/msystems.00250-24
75. Ravi, J., Anantharaman, V., Chen, S. Z., Brenner, E. P., Datta, P., Aravind, L., & Gennaro, M. L. (2024). The phage shock protein (PSP) envelope stress response: discovery of novel partners and evolutionary history. *MSystems*, *9*(6). https://doi.org/10.1128/msystems.00847-23
76. Richardson, A. E., Lynch, J. P., Ryan, P. R., Delhaize, E., Smith, F. A., Smith, S. E., Harvey, P. R., Ryan, M. H., Veneklaas, E. J., Lambers, H., Oberson, A., Culvenor, R. A., & Simpson, R. J. (2011). Plant and microbial strategies to improve the phosphorus efficiency of agriculture. *Plant and Soil*, *349*(1–2), 121–156. https://doi.org/10.1007/s11104-011-0950-4
77. Robinson, J. T., Thorvaldsdóttir, H., Winckler, W., Guttman, M., Lander, E. S., Getz, G., & Mesirov, J. P. (2011). Integrative genomics viewer. *Nature Biotechnology*, *29*(1), 24–26. https://doi.org/10.1038/nbt.1754
78. Sano, S., Aoyama, M., Nakai, K., Shimotani, K., Yamasaki, K., Sato, M. H., Tojo, D., Suwastika, I. N., Nomura, H., & Shiina, T. (2014). Light-dependent expression of flg22-induced defense genes in Arabidopsis. *Frontiers in Plant Science*, *5*. https://doi.org/10.3389/fpls.2014.00531
79. Schneider, C. A., Rasband, W. S., & Eliceiri, K. W. (2012). NIH Image to ImageJ: 25 years of image analysis. *Nature Methods*, *9*(7), 671–675. https://doi.org/10.1038/nmeth.2089
80. Seef, S., Herrou, J., de Boissier, P., My, L., Brasseur, G., Robert, D., Jain, R., Mercier, R., Cascales, E., Habermann, B. H., & Mignot, T. (2021). A tad-like apparatus is required for contact-dependent prey killing in predatory social bacteria. *ELife*, *10*. https://doi.org/10.7554/eLife.72409
81. Sessitsch, A., Hardoim, P., Döring, J., Weilharter, A., Krause, A., Woyke, T., Mitter, B., Hauberg-Lotte, L., Friedrich, F., Rahalkar, M., Hurek, T., Sarkar, A., Bodrossy, L., Van Overbeek, L., Brar, D., Van Elsas, J. D., & Reinhold-Hurek, B. (2012). Functional Characteristics of an Endophyte Community Colonizing Rice Roots as Revealed by Metagenomic Analysis. *Molecular Plant-Microbe Interactions*, *25*(1), 28–36. https://doi.org/10.1094/MPMI
82. Sorokan, A., Cherepanova, E., Burkhanova, G., Veselova, S., Rumyantsev, S., Alekseev, V., Mardanshin, I., Sarvarova, E., Khairullin, R., Benkovskaya, G., & Maksimov, I. (2020). Endophytic Bacillus spp. as a Prospective Biological Tool for Control of Viral Diseases and Non-vector Leptinotarsa decemlineata Say. in Solanum tuberosum L. *Frontiers in Microbiology*, *11*. https://doi.org/10.3389/fmicb.2020.569457
83. Spaepen, S., & Vanderleyden, J. (2011). Auxin and plant-microbe interactions. *Cold Spring Harbor Perspectives in Biology*, *3*(4), 1–13. https://doi.org/10.1101/cshperspect.a001438
84. Taboada, B., Estrada, K., Ciria, R., & Merino, E. (2018). Operon-mapper: A web server for precise operon identification in bacterial and archaeal genomes. *Bioinformatics*, *34*(23), 4118–4120. https://doi.org/10.1093/bioinformatics/bty496

85. Tatusova, T., Dicuccio, M., Badretdin, A., Chetvernin, V., Nawrocki, E. P., Zaslavsky, L., Lomsadze, A., Pruitt, K. D., Borodovsky, M., & Ostell, J. (2016). NCBI prokaryotic genome annotation pipeline. *Nucleic Acids Research*, *44*(14), 6614–6624. https://doi.org/10.1093/nar/gkw569

86. Timmusk, S., Grantcharova, N., & Wagner, E. G. H. (2005). Paenibacillus polymyxa invades plant roots and forms biofilms. *Applied and Environmental Microbiology*, *71*(11), 7292–7300. https://doi.org/10.1128/AEM.71.11.7292-7300.2005

87. Tzipilevich, E., Russ, D., Dangl, J. L., & Benfey, P. N. (2021). Plant immune system activation is necessary for efficient root colonization by auxin-secreting beneficial bacteria. *Cell Host and Microbe*, *29*(10), 1507-1520.e4. https://doi.org/10.1016/j.chom.2021.09.005

88. Uwaremwe, C., Yue, L., Wang, Y., Tian, Y., Zhao, X., Liu, Y., Zhou, Q., Zhang, Y., & Wang, R. (2022). An Endophytic Strain of Bacillus amyloliquefaciens Suppresses Fusarium oxysporum Infection of Chinese Wolfberry by Altering Its Rhizosphere Bacterial Community. *Frontiers in Microbiology*, *12*. https://doi.org/10.3389/fmicb.2021.782523

89. Vaser, R., & Šikić, M. (2021). Time- and memory-efficient genome assembly with Raven. *Nature Computational Science*, *1*(5), 332–336. https://doi.org/10.1038/s43588-021-00073-4

90. Veselova, S. V., Sorokan, A. V., Burkhanova, G. F., Rumyantsev, S. D., Cherepanova, E. A., Alekseev, V. Y., Sarvarova, E. R., Kasimova, A. R., & Maksimov, I. V. (2022). By Modulating the Hormonal Balance and Ribonuclease Activity of Tomato Plants Bacillus subtilis Induces Defense Response against Potato Virus X and Potato Virus Y. *Biomolecules*, *12*(2). https://doi.org/10.3390/biom12020288

91. Weselowski, B., Nathoo, N., Eastman, A. W., MacDonald, J., & Yuan, Z. C. (2016). Isolation, identification and characterization of Paenibacillus polymyxa CR1 with potentials for biopesticide, biofertilization, biomass degradation and biofuel production. *BMC Microbiology*, *16*(1). https://doi.org/10.1186/s12866-016-0860-y

92. White, J. F., Kingsley, K. L., Zhang, Q., Verma, R., Obi, N., Dvinskikh, S., Elmore, M. T., Verma, S. K., Gond, S. K., & Kowalski, K. P. (2019). Review: Endophytic microbes and their potential applications in crop management. *Pest Management Science*, *75*(10), 2558–2565. https://doi.org/10.1002/ps.5527

93. Wick, R. R., & Holt, K. E. (2022). Polypolish: Short-read polishing of long-read bacterial genome assemblies. *PLoS Computational Biology*, *18*(1). https://doi.org/10.1371/journal.pcbi.1009802

94. Wick, R. R., Judd, L. M., Cerdeira, L. T., Hawkey, J., Méric, G., Vezina, B., Wyres, K. L., & Holt, K. E. (2021). Trycycler: consensus long-read assemblies for bacterial genomes. *Genome Biology*, *22*(1). https://doi.org/10.1186/s13059-021-02483-z

95. Wittstock, U., & Burow, M. (2010). Glucosinolate Breakdown in Arabidopsis: Mechanism, Regulation and Biological Significance. *The Arabidopsis Book*, *8*, e0134. https://doi.org/10.1199/tab.0134

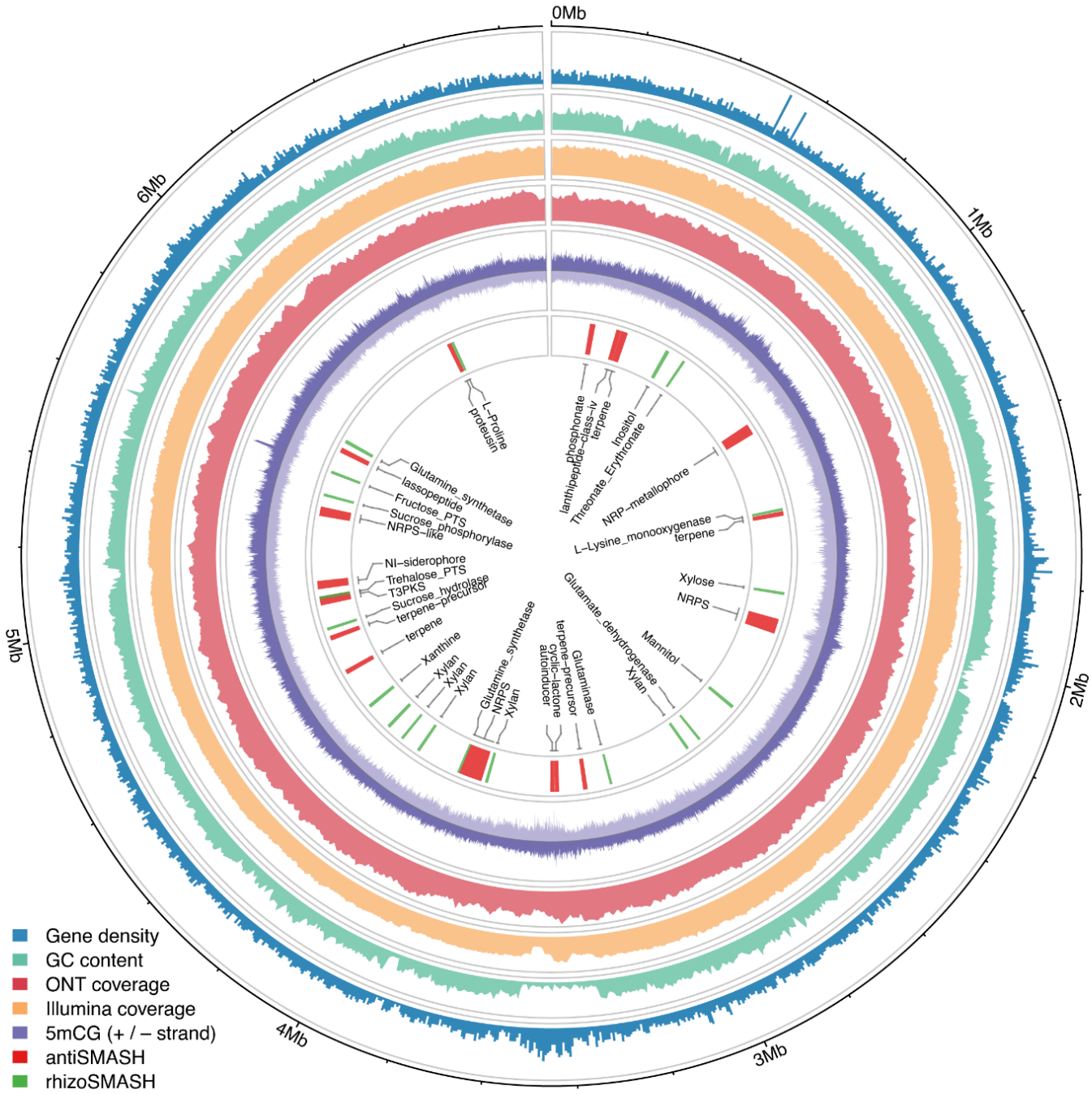
96. Yang, P., Yuan, P., Liu, W., Zhao, Z., Bernier, M. C., Zhang, C., Adhikari, A., Opiyo, S. O., Zhao, L., Banks, F., & Xia, Y. (2024). Plant Growth Promotion and Plant Disease Suppression Induced by Bacillus amyloliquefaciens Strain GD4a. *Plants*, *13*(5). https://doi.org/10.3390/plants13050672

97. Yuan, C., Ruan, L., Yang, Y., Wang, L., Ke, Z., & He, J. (2025). Paenibacillus wuxiensis sp. nov., a Novel Bacterium Capable of Producing Indole-3-Acetic Acid (IAA) and Inhibiting Rhizoctonia solani Kühn

Isolated from Agricultural Soil. *Current Microbiology*, *82*(11). https://doi.org/10.1007/s00284-025-04502-9

98. Zhou, J. Y., Zhao, X. Y., & Dai, C. C. (2014). Antagonistic mechanisms of endophytic *Pseudomonas fluorescens* against *Athelia rolfsii*. *Journal of Applied Microbiology*, *117*(4), 1144–1158. https://doi.org/10.1111/jam.12586

# Figures



## Figure 1

**Organisation of *Paenibacillus* sp. ST1 genome.** Circos plot from outer to inner rings: gene density, GC content (%), Illumina read coverage, ONT read coverage, ONT 5mCG methylation calls, and biosynthetic gene clusters identified by antiSMASH and plant growth promotion related clusters by rhizoSMASH (cluster names given in the middle). Coordinates are shown in megabases (Mb).

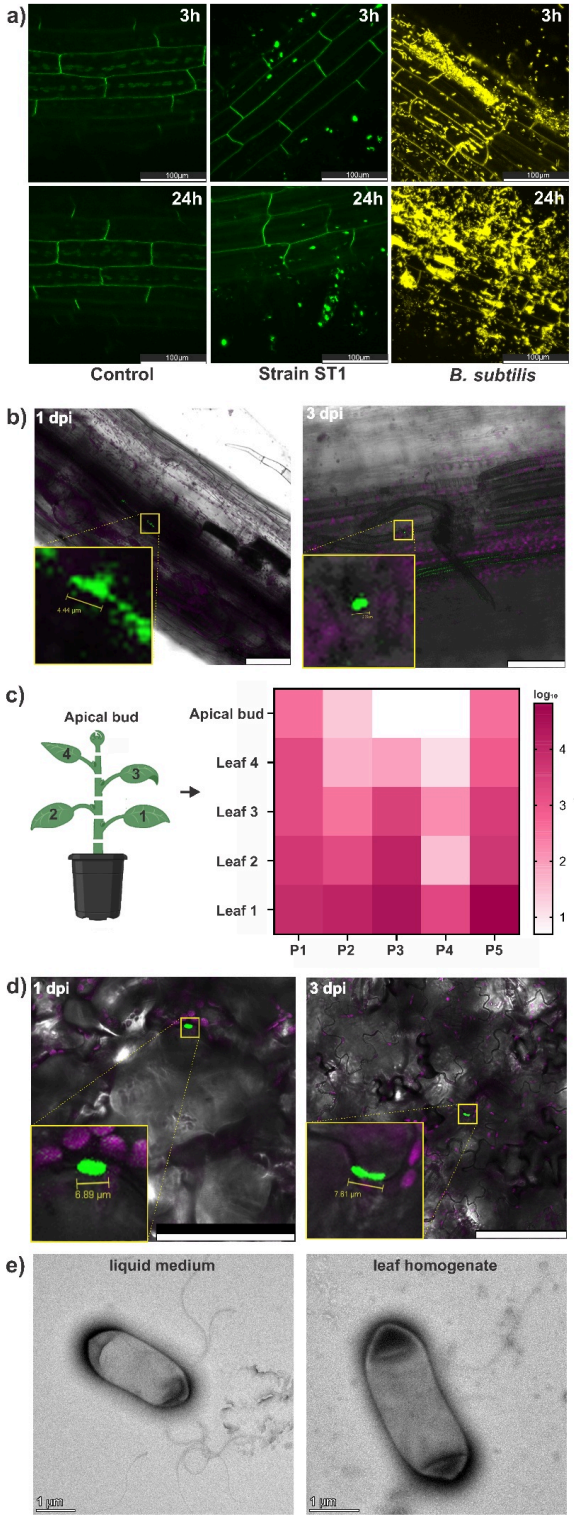
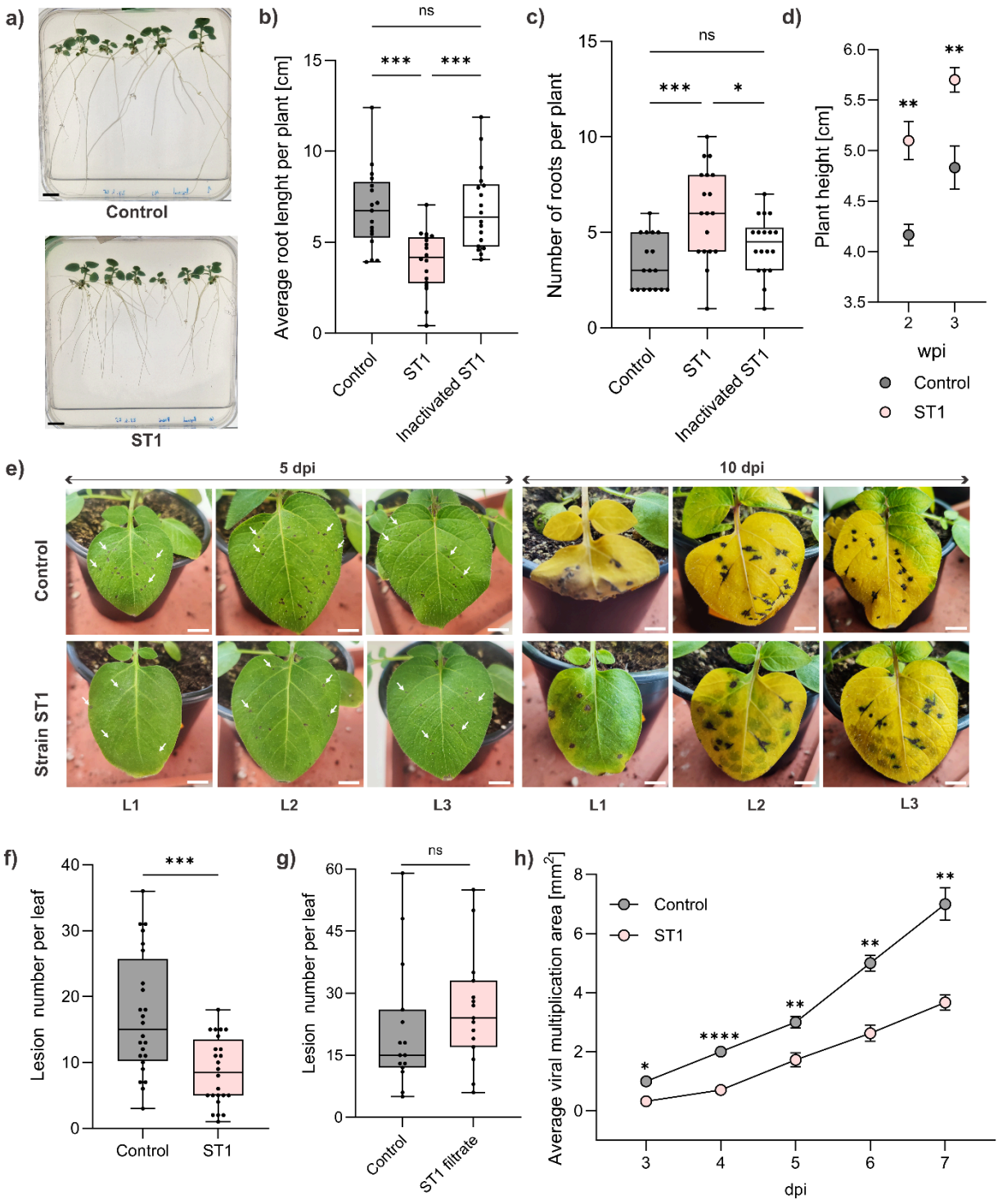


**Figure 2**

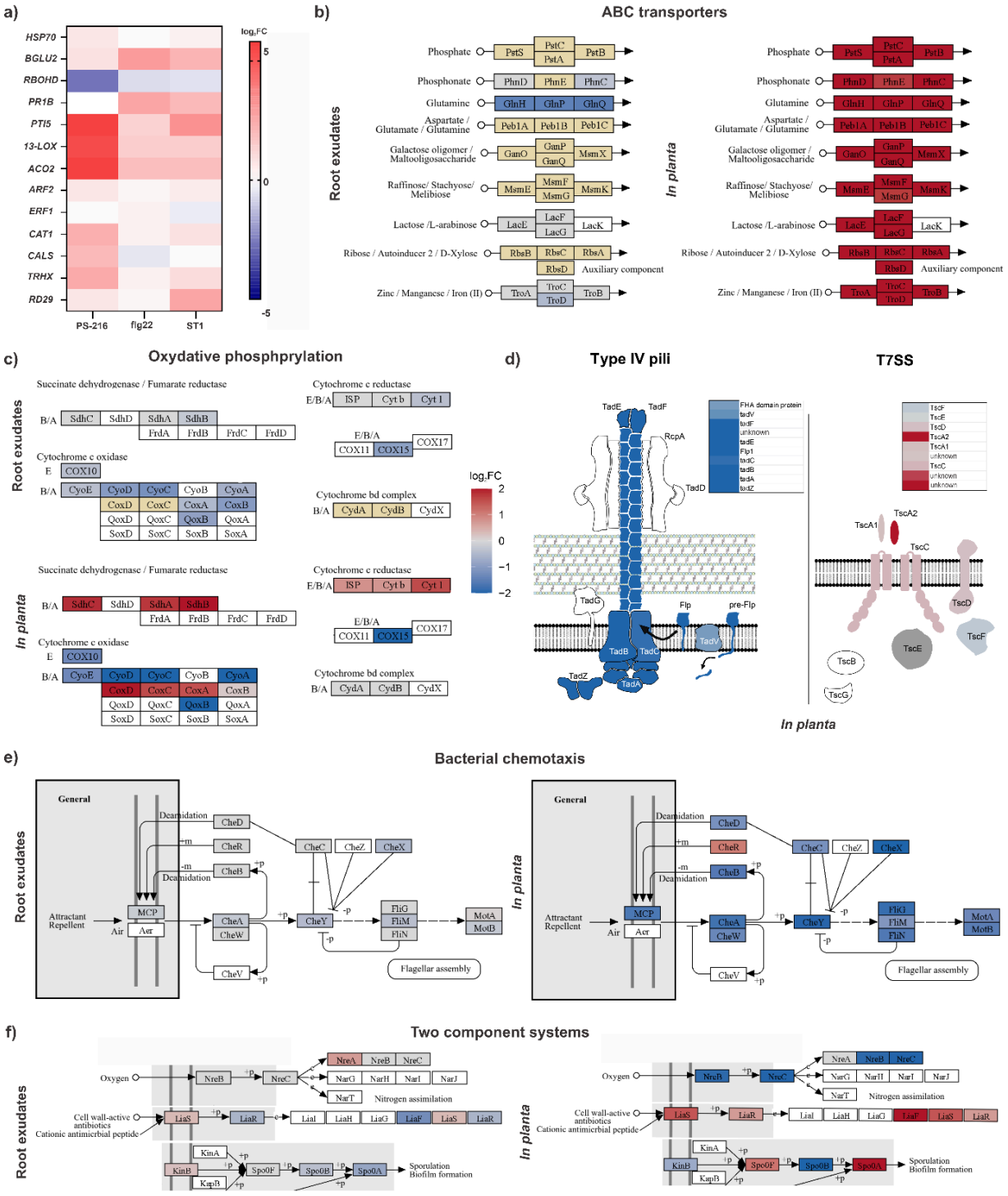
***Paenibacillus* sp. ST1 colonises the whole potato plant**. a) Strain ST1 adheres to potato roots but does not form biofilm. Representative root images of Rywal after 3 h and 24 h of incubation with bacterial strain ST1, *B. subtilis* PS-216 or in medium without bacteria (control). The tagged strain ST1 was visualized in the GFP channel (green), while tagged *B. subtilis* was visualized in the YFP channel (yellow). Scale bar represents 100 µm. b) Strain ST1 was detected in xylem of leaf petiole and of upper stem at 1 dpi. The GFP-tagged strain ST1 is shown in green (GFP channel). Chlorophyll autofluorescence is shown in purple (RFP channel). Scale bar represents 100 µm. Sizes in inset images are 4.4 µm (1 dpi) and 2.9 µm (3 dpi). c) Relative abundance of strain ST1 in different plant tissues, from lower leaves to the apical bud at 7 dpi. P1–P5 represent individual plants used as biological replicates. Bacterial relative abundance values were normalized and $\log_{10}$-transformed for visualization; darker colors indicate higher relative abundance. Adapted from BioRender.com. d) Strain ST1 colonization of plant tissues does not alter morphology of bacteria. Localization and morphology of strain ST1 at 1 and 3 days after leaf infiltration as determined by confocal microscopy. The GFP-tagged strain ST1 is shown in green. Chlorophyll autofluorescence is shown in purple. Scale bar represents 100 µm. Sizes in inset images are 6.9 µm (1 dpi) and 7.6 µm (3 dpi). e) TEM comparison of bacterial morphology in liquid medium before infiltration (left) and of bacteria from leaf homogenate 3 days post infiltration (right), supporting the observations in panel (d). Scale bar represents 1 µm. Original images are available in the accompanying Zenodo dataset.




## Figure 3

**Interaction of plant with *Paenibacillus* sp. ST1 improves drought tolerance and enhances protection against viral infection.** a) Potato plants grown on different media showing differences in root architecture after 14 days of growth. Scale bar represents 1 cm. b) Average root length per plant (cm) grown in media with viable bacteria ($10^4$–$10^6$ CFU/mL), inactivated bacteria or with no bacteria added (control). Each data point represents the mean root length of one plant. Roots were measured after 14

days of growth; n = 17-18 plants per group. Statistical significance was determined by one-way ANOVA followed by Šídák's multiple comparisons test; *** $p < 0.001$, ns - not significant. c) Number of roots per plant grown in media with viable bacteria, inactivated bacteria or with no bacteria added (control). Each data point represents the number of roots of one plant. Boxplots indicate the median and interquartile range; whiskers extend from minimum to maximum values. Roots were counted after 14 days of growth; n = 17-18 plants per group. Statistical significance was determined by one-way ANOVA followed by Holm-Šídák's multiple comparisons test; *** $p < 0.001$, * $p < 0.05$, ns - not significant. d) Effect of strain ST1 on Rywal height in drought. Plants inoculated with ST1 showed significantly increased height compared to control plants at 2 and 3 weeks post inoculation (wpi). Points represent mean ± SEM. Statistical significance was determined by an unpaired t-test with Welch's correction; ** $p < 0.01$. e) Development of symptoms on leaves of susceptible potato genotype on three sequential leaves. NahG-Rywal leaves at 5 and 10 days post PVY infection following pre-inoculation with strain ST1 infiltration or solution treated control. Scale bar = 1 cm. f) Comparison of lesion number per infected leaf between ST1-treated plants and control at 5 dpi. Each data point represents one infected leaf. Statistical significance was determined by unpaired t-test with Welch's correction due to unequal variances; *** $p < 0.001$; n = 24 leaves per group. g) Comparison of lesion number per infected leaf between ST1 filtrate treated plants and control at 5 dpi. Each data point represents one infected leaf. Boxplots indicate the median and interquartile range; whiskers extend from minimum to maximum values. Statistical significance was determined by unpaired t-test; ns - not significant ($p \geq 0.05$); n = 15 leaves per group. h) Viral multiplication is attenuated in strain ST1 inoculated in *N. tabacum*. Comparison of average viral multiplication area ($mm^2$) between ST1-treated plants and non-treated inoculated plants (control). Data represent mean viral area per plant per day, calculated from 6 measurements. Data are presented as mean ± SEM. Statistical analysis was performed using a mixed-effects model (REML), with treatment and time as fixed effects and plant as a random effect (n = 6 plants per group); * $p < 0.05$, ** $p < 0.01$, **** $p < 0.0001$.




## Figure 4

**Plant immune responses and strain ST1 transcriptional adaptation during plant–bacteria interaction.** a) Differences in gene expression of immune response marker genes in potato roots following different stimuli, including flagellin (flg22) treatment and inoculation with *B. subtilis* PS-216 or strain ST1. Non-inoculated plants served as controls. Full dataset with results of statistical analysis is available in Table S4. b–f) Differentially expressed KEGG pathways in strain ST1 under different plant-associated

conditions. KEGG pathway maps show significantly regulated genes (|log2FC| ≥ 1, adjusted p ≤ 0.05) in (b) ABC transporters (c) oxidative phosphorylation, (d) type IV pili and T7SS, (e) bacterial chemotaxis and (f) two component systems. Red boxes indicate upregulated genes, blue boxes indicate downregulated genes, and yellow boxes indicate little or no change relative to the control condition. Colour intensity reflects the magnitude of log2 fold change. Complete dataset is available in Table S6.

## Supplementary Files

This is a list of supplementary files associated with this preprint. Click to download.

- SupplementaryFigures.docx
- SupplementaryTables.xlsx
- SupplementaryMethods.docx